Bioconjugate Chemistry

Article

pubs.acs.org/bc

^{99m}Tc-Labeled 2-Arylbenzothiazoles: Aβ Imaging Probes with Favorable Brain Pharmacokinetics for Single-Photon Emission Computed Tomography

Xiaoyang Zhang,[†] Pingrong Yu,[†] Yanping Yang,[†] Yaqin Hou,[‡] Cheng Peng,[‡] Zhigang Liang,[*,‡] Jing Lu,[§] Baian Chen,[*,§] Jiapei Dai,[∥] Boli Liu,[†] and Mengchao Cui[*,†]

[†]Key Laboratory of Radiopharmaceuticals, Ministry of Education, Beijing Normal University, Beijing 100875, China

[‡]Department of Nuclear Medicine, Xuanwu Hospital, Capital Medical University, Beijing 100053, China

[§]Department of Laboratory Animal Science, School of Basic Medical Science, Capital Medical University, Beijing 100069, China

[∥]Wuhan Institute for Neuroscience and Neuroengineering, South-Central University for Nationalities, Wuhan 430074, China

Supporting Information

ABSTRACT: A series of 2-arylbenzothiazole derivatives conjugated with bis(aminoethanethiol) (BAT) chelating groups were designed and synthesized. A competitive binding assay-based screening was used to select seven rhenium complexes with potent binding affinity toward $A\beta_{1-42}$ aggregates (K_i < 50 nM) for ^{99m}Tc labeling and further evaluation. The ^{99m}Tc-labeled probes showed good affinity and specificity to Aβ plaques in Tg mouse brain tissue in in vitro autoradiography studies. Moreover, [^{99m}Tc]**14b** exhibited favorable brain pharmacokinetics in normal mice (2.11% ID/g at 2 min and 0.62% ID/g at 60 min). Ex vivo autoradiography revealed extensive labeling of Aβ plaques by [^{99m}Tc]**14b** in the brain of Tg mice. Furthermore, we performed the first single-photon emission computed tomography (SPECT) imaging study in nonhuman primates with ^{99m}Tc-labeled Aβ probes. The semiquantitative data showed that [^{99m}Tc]**14b** penetrated the brains of rhesus monkeys. These results indicate that [^{99m}Tc]**14b** could be utilized as a SPECT imaging probe for Aβ plaques.

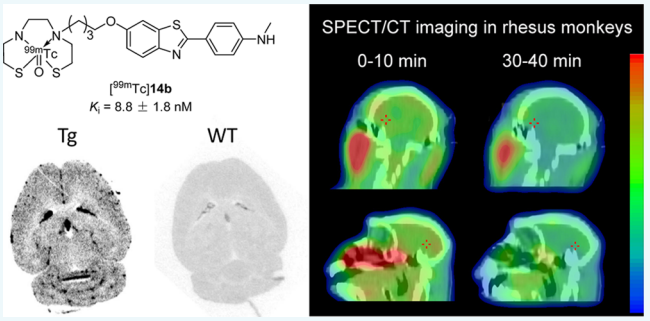

INTRODUCTION

Alzheimer's disease (AD) is a common, devastating neurodegenerative disease that is the most prevalent type of dementia.[1,2] According to Alzheimer's Disease International, there were estimated 46.8 million people with dementia worldwide in 2015; this number is expected to reach 131.5 million by 2050.[3] Currently available methods of definitively diagnosing AD can only be performed postmortem. Very few methods have been found to be effective in treating AD symptoms or halting the progression of the disease.[4,5] The significant burden of AD on patients, their families, and their societies necessitates the development of effective diagnostic and therapeutic strategies.

As a pathological hallmark of the AD-afflicted brain, Aβ plaques have been the target of diagnosis methods for decades.[6−8] Nuclear imaging technologies, including positron emission tomography (PET) and SPECT, are promising methods of visualizing Aβ plaques. For PET, many radiolabeled molecular probes have been investigated as means of imaging Aβ plaques.[9] A total of three PET imaging agents (Amyvid,[10] Vizamyl,[11] and Neuraceq[12]) have been approved by the United States Food and Drug Administration (FDA), but the development of imaging probes for SPECT has been far slower.[8,13] Only a few radio-iodinated SPECT imaging agents have been tested in humans, including [^{123}I]IMPY (6-iodo-2-(4′-dimethylamino)phenyl-imidazo[1,2-*a*]-pyridine)[14] and [^{123}I]ABC577.[15]

SPECT imaging has several advantages over PET imaging, including the capacity to utilize technetium-99m (^{99m}Tc), an artificial isotope with an ideal half-life and radiation energy emission properties, which is available from generators.[16] SPECT imaging agents targeting Aβ plaques will be particular use in developing countries where PET facilities are rare. To introduce ^{99m}Tc into imaging molecules, chelating groups are necessarily added to binding scaffolds by conjugate[17−19] or integrated[20−23] approaches (Figure 1). Although many efforts have been made to develop ^{99m}Tc-labeled probes for imaging Aβ plaques, no candidate probe has been found to possess both high binding affinity and suitable in vivo characteristics, especially sufficient brain uptake and rapid excretion from the

Received: August 9, 2016
Revised: September 21, 2016

DOI: 10.1021/acs.bioconjchem.6b00444
Bioconjugate Chem. XXXX, XXX, XXX−XXX

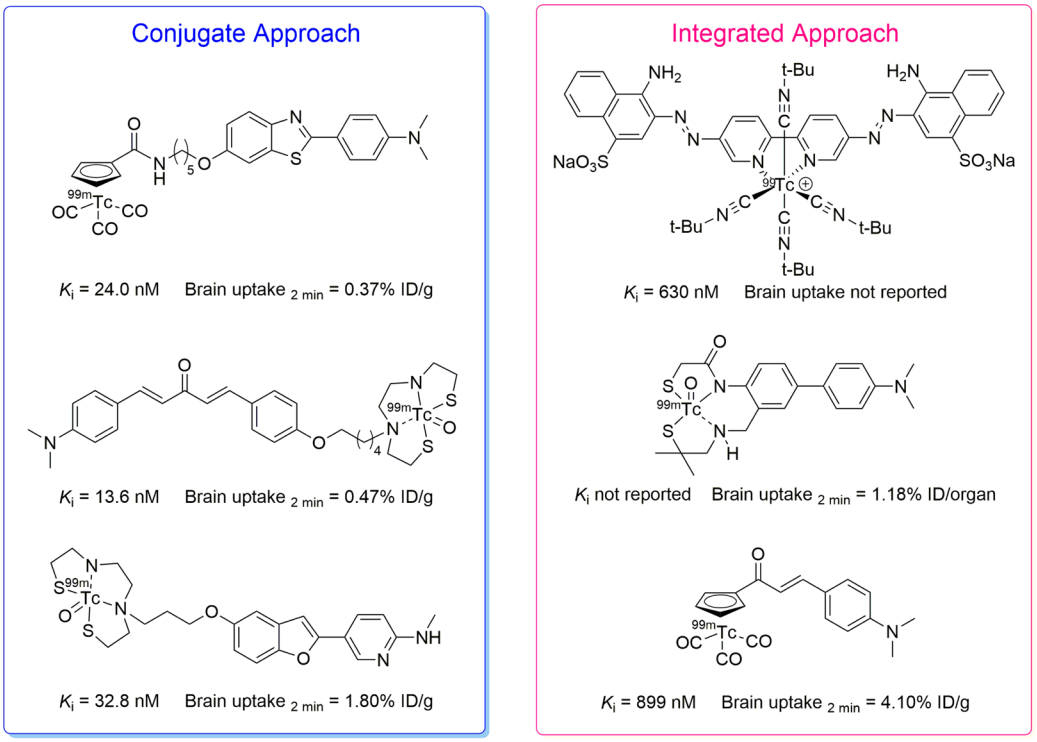

Figure 1. Chemical structures and biological properties of ^{99m}Tc-labeled Aβ imaging probes designed by different strategies.

normal brain.[8] Many reported ^{99m}Tc/Re-labeled probes were not fully evaluated or even radiolabeled. Probes designed through conjugate approach readily maintained potent binding affinity for Aβ plaques, but their initial brain uptake was insufficient. Ono et al. reported ^{99m}Tc-labeled pyridyl benzofuran derivatives conjugated to a bis(aminoethanethiol) (BAT) chelating ligand and showed that [^{99m}Tc]BAT−Bp-2, containing a monomethyl amino group, had sufficient binding affinity for Aβ_{1-42} aggregates and initial brain uptake of 1.80% ID/g at 2 min post-injection; this is the greatest reported initial brain uptake for a ^{99m}Tc-labeled Aβ probe designed by conjugation.[19] Unfortunately, no further reports of the clinical utility of [^{99m}Tc]BAT-Bp-2 were published. In contrast, probes designed via integrated approach possessing high initial brain uptake were unable to keep the efficient binding affinity for Aβ plaques. Li et al. reported three ^{99m}Tc-labeled chalcone derivatives through integrated approach, in which one phenyl group of chalcone was replaced by the Cp^{99m}Tc(CO)$_3$ core (Cp = cyclopentadienyl). The probe with one double bond exhibited very high brain uptake (4.10% ID/g at 2 min) but poor affinity for Aβ_{1-42} aggregates (K_i = 899 nM).

In this work, we designed and synthesized a series of ^{99m}Tc-labeled imaging probes for Aβ plaques through the conjugate approach. 2-Arylenzothiazole, a classical Aβ binding structure,[24] was chosen as a chemical scaffold to confer binding affinity for Aβ plaques. Considering its relatively good BBB permeability, BAT was conjugated to the scaffold as a chelating group for ^{99m}Tc.[25−27] Mono methyl or dimethylamino moieties and alkyl linkers of different length were employed to adjust the molecular lipophilicity and balance the binding affinity and BBB permeability of the imaging probes. The purpose of this study was to identify potential SPECT imaging probes for Aβ plaques with potent binding affinity and also favorable brain pharmacokinetics.

RESULTS AND DISCUSSION

Chemistry. The synthesis of 2-arylbenzothiazole derivatives is outlined in Scheme 1. A total of four types of 2-arylbenzothiazole scaffolds (**1**−**4**) were readily prepared as previously reported, followed by a Williamson reaction with one terminal of 1,*m*-dibromoalkane (*m* = 3, 4, 5, and 6). Next, the obtained bromine compounds (**5a**−**d**, **6a**−**d**, **7a**−**d**, and **8a**−**d**) were successfully conjugated to the *N*-Boc- and *S*-Tr-protected BAT chelating group using KI and K_2CO_3 in acetonitrile, producing precursors for ^{99m}Tc labeling (**9a**−**d**, **10a**−**d**, **11a**−**d**, and **12a**−**d**). As nonradioactive surrogates for ^{99m}Tc complexes, rhenium complexes (**13a**−**d**, **14a**−**d**, **15a**−**d**, and **16a**−**d**) were synthesized by reaction of the deprotected precursors and $(PPh_3)_2ReOCl_3$.

Scheme 1. Synthesis of 2-Arylbenzothiazole Derivatives[a]

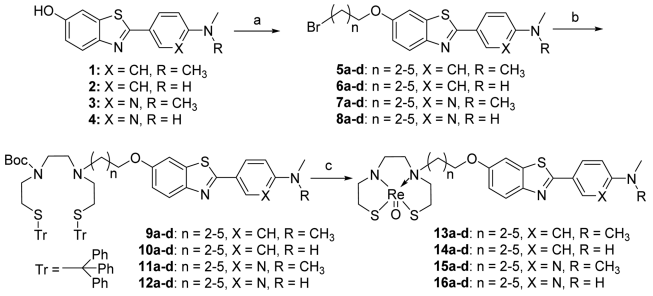

[a]Reagents and conditions: (a) 1,*m*-dibromoalkane (*m* = 3, 4, 5, and 6), K_2CO_3, CH_3CN, 90 °C; (b) BAT−Boc, KI, K_2CO_3, CH_3CN, 90 °C; (c) (i) TFA, Et_3SiH; (ii) $(PPh_3)_2ReOCl_3$, NaOAc, CH_2Cl_2, MeOH, 90 °C.

In Vitro Binding Assay Using Aggregated Aβ_{1-42} Peptides. The binding affinity of each rhenium complex was quantitatively evaluated by competitive binding assay using

DOI: 10.1021/acs.bioconjchem.6b00444
Bioconjugate Chem. XXXX, XXX, XXX−XXX

[^{125}I]IMPY as a reference ligand. IMPY was also tested under the same assay conditions for comparison. The K_i values of the 16 rhenium complexes ranged from 8.4 to 2356.2 nM (Table 1). Most complexes with an *N,N*-dimethylamino group

Table 1. Inhibition Constants (K_i) for Binding of [^{125}I]IMPY to Aβ_{1-42} Aggregates

compound	X	R	*n*	K_i (nM)[a]
13a	CH	CH_3	2	56.6 ± 17.3
13b	CH	CH_3	3	16.0 ± 5.7
13c	CH	CH_3	4	33.5 ± 18.4
13d	CH	CH_3	5	8.4 ± 0.7
14a	CH	H	2	2303.0 ± 581.1
14b	CH	H	3	8.8 ± 1.8
14c	CH	H	4	104.9 ± 20.7
14d	CH	H	5	29.4 ± 14.3
15a	N	CH_3	2	105.6 ± 25.2
15b	N	CH_3	3	134.1 ± 66.1
15c	N	CH_3	4	17.6 ± 12.9
15d	N	CH_3	5	24.4 ± 2.8
16a	N	H	2	2356.2 ± 1178.6
16b	N	H	3	93.6 ± 31.7
16c	N	H	4	440.9 ± 133.6
16d	N	H	5	75.4 ± 20.2
IMPY	–	–	–	12.6 ± 1.1

[a]Measured in triplicate with results presented as the mean ± SD.

exhibited binding affinity greater than that of complexes with a monomethylamino group. Several studies have found that *N,N*-dimethylamino groups confer Aβ aggregate binding affinity.[17,28,29] The relatively long alkyl chains between the benzothiazole scaffold and the BAT chelating ligand also increased binding affinity; the interaction of the binding scaffold and the Aβ aggregates was less influenced by the conjugated BAT group. A total of seven rhenium complexes demonstrating potent binding to Aβ_{1-42} peptides (K_i < 50 nM) were selected for radiolabeling and further investigation. The binding affinity of the benzothiazole scaffold was mostly maintained by the tested rhenium complexes. Compounds **13d** and **14b** showed nanomolar binding affinity (8.4 and 8.8 nM, respectively), which was better than that of IMPY (12.6 nM) and BAT−Bp-2 (32.8 nM).[19]

In Vitro Fluorescent Staining of Aβ Plaques in Tg Mice and AD Brains. Fluorescent staining of the selected rhenium complexes was performed on brain slices from Tg mice and AD patients. In Tg mouse brain tissue, clear fluorescent spots were observed after incubation with each of the seven rhenium complexes. Similar staining patterns were observed in adjacent slices stained with thioflavin-S (Figures 2 and S1). Furthermore, senile plaques were clearly stained by **13d** and **14b** in brain tissue from three AD patients (Figure 2); the other five rhenium complexes also stained Aβ plaques in human brain tissue (Figure S2). These results indicate that the selected rhenium complexes bind specifically to Aβ plaques in brain tissue from Tg mice and AD patients.

Radiochemistry. To prepare ^{99m}Tc-labeled complexes, a ligand exchange reaction with ^{99m}Tc−glucoheptonate (^{99m}Tc−GH) was employed. The precursors were first deprotected by trifluoroacetic acid and triethylsilane, after which they were reacted with newly prepared ^{99m}Tc−GH at 100 °C for 10 min (Scheme 2). The desired ^{99m}Tc-labeled products were purified via radio-HPLC (radiochemical purity >95%) and identified by

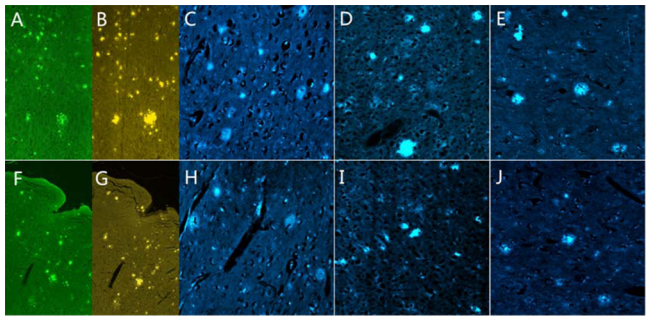

Figure 2. In vitro fluorescent staining of Aβ plaques by **13d** (A−E) and **14b** (F−J) in brain slices from Tg mice (APPswe/PSEN1, male, 12 months old; A and F stained by rhenium complexes, B and G stained by thioflavin-S) and three AD patients (C and H: 64 years old, female, temporal lobe; D and I: 91 years old, male, temporal lobe; E and J: 68 years old, female, temporal lobe).

Scheme 2. Preparation of ^{99m}Tc-labeled Complexes[a]

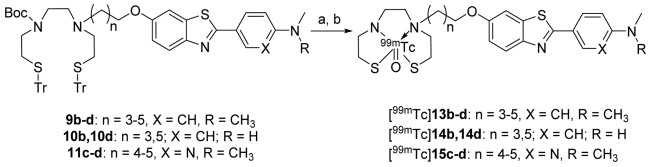

[a]Reagents and conditions: (a) TFA, Et_3SiH, rt, 10 min; (b) ^{99m}Tc−GH, 100 °C, 10 min.

retention time comparison using the corresponding rhenium complexes (Figure S3). The overall radiochemical yield ranged from 61% to 97% when the radiolabeling condition was not optimized, which demonstrates the suitability for kit formulation and clinical diagnostic imaging. Additionally, [^{99m}Tc]**14b** was stable in saline for 6 h at room temperature (purity: 95.6%) and also stable in mice serum for 1 h at 37 °C (purity: 95.4%) (Figure S4).

In Vitro Autoradiography. The capacity of the purified ^{99m}Tc-labeled probes to bind Aβ plaques was tested in brain slices from Tg mice. The autoradiography images of the cerebral cortex revealed radioactive areas, which were confirmed as Aβ plaques by fluorescent staining of the same slices with DANIR-3b[30] (Figures 3 and S5). No Aβ plaques were detected in the brain slices from wild-type mice. The effective labeling of Aβ plaques demonstrated the potent binding affinity and specificity of the ^{99m}Tc-labeled probes. These results were consistent with the fluorescent staining and low K_i values of the corresponding rhenium complexes.

Biodistribution in Normal Mice. BBB penetration is critical for imaging probes intended for use in the brain. High initial brain uptake and rapid clearance from normal brain tissue are desirable characteristics for probes in primary biodistribution studies. Biodistribution of ^{99m}Tc-labeled complexes were assessed in normal ICR mice (18−22 g, male). The brain uptake profile of [^{99m}Tc]**14b** (Table 2 and Figure 4) indicated its suitability as a diagnostic probe; [^{99m}Tc]**14b** showed relatively high initial brain uptake (2.11% ID/g at 2 min) and a reasonable clearance rate (0.62% ID/g at 60 min), while the other complexes exhibited poor brain uptake (less than 1% ID/g at 2 min) and slow clearance, perhaps because these compounds were more lipophilic and thus subject to more nonspecific binding to plasma proteins. A trend was observed for the seven probes discussed in this section: initial brain

DOI: 10.1021/acs.bioconjchem.6b00444
Bioconjugate Chem. XXXX, XXX, XXX−XXX

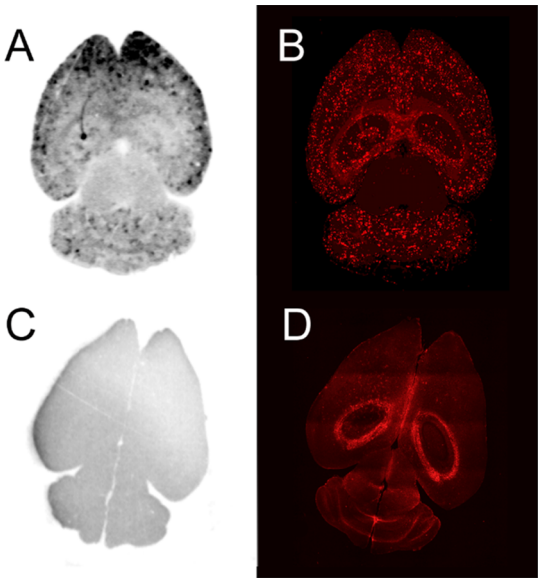

Figure 3. In vitro autoradiography of [^{99m}Tc]**14b** in brain slices (A and C) from a Tg mouse (APPswe/PSEN1, male, 12 months old) and a wild-type mouse (C57BL6, male, 12 months old). The same brain slices were subsequently fluorescent stained with DANIR-3b (B and D).

Table 2. Brain Uptake of [^{99m}Tc] Tracers after Intravenous Administration to Normal ICR Mice (Mean ± SD, n = 5)[a] and the Retention Time of [^{99m}Tc] Tracers in Radio-HPLC[b]

compound	2 min	60 min	ratio$_{2\ min/60\ min}$	retention time (min)
[^{99m}Tc] **13b**	0.69 ± 0.16	0.46 ± 0.12	1.50	13.91
[^{99m}Tc] **13c**	0.46 ± 0.09	0.40 ± 0.09	1.15	17.18
[^{99m}Tc] **13d**	0.59 ± 0.12	0.43 ± 0.15	1.37	19.87
[^{99m}Tc] **14b**	2.11 ± 0.11	0.62 ± 0.08	3.40	8.81
[^{99m}Tc] **14d**	0.92 ± 0.09	0.63 ± 0.15	1.46	12.59
[^{99m}Tc] **15c**	0.47 ± 0.07	0.19 ± 0.03	2.47	12.48
[^{99m}Tc] **15d**	0.60 ± 0.05	0.29 ± 0.05	2.07	15.50

[a]Expressed as percent injected dose per gram. [b]HPLC analysis conditions: Venusil MP C18 column (Bonna-Agela Technologies, 5 μm, 4.6 × 250 mm); CH_3CN-H_2O = 80%:20%; flow rate, 1 mL/min.

uptake and clearance rate were both reduced when the HPLC retention time of the ^{99m}Tc-labeled complex was increased (Figure 4B,C). It is notable that [^{99m}Tc]**14b** had the shortest radio-HPLC retention time, indicating relatively low lipophilicity. In addition to lipophilicity, the brain uptake of radiotracers depends on many different factors, which cannot be fully explained in this study. Although the initial brain uptake of [^{99m}Tc]**14b** was still much less than that of [^{18}F]AV-45 (7.33% ID/g at 2 min),[31] it was comparable to that of [^{123}I]IMPY (2.88% ID/g at 2 min)[32] and greater than that of [^{99m}Tc]BAT−Bp-2 (1.80% ID/g at 2 min)[19] and other ^{99m}Tc-labeled Aβ probes reported in previous studies.[8] The clearance ratio$_{2\ min/60\ min}$ (3.40) was close to that of [^{18}F]AV-45 (3.90) and better than that of [^{99m}Tc]BAT−Bp-2 (2.28). These are the most encouraging brain uptake results ever reported for a

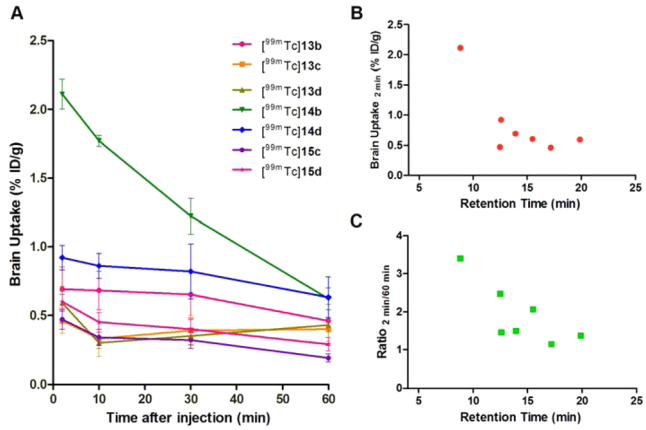

Figure 4. (A) Brain pharmacokinetics of [^{99m}Tc]tracers in normal ICR mice (mean ± SD, n = 5); (B) correlation between the initial brain uptake and retention time of [^{99m}Tc]tracers in radio-HPLC; (C) correlation between the brain clearance rate and retention time of [^{99m}Tc]tracers in radio-HPLC. HPLC analysis conditions: Venusil MP C18 column (Bonna-Agela Technologies, 5 μm, 4.6 × 250 mm); CH_3CN-H_2O = 80%:20%; flow rate, 1 mL/min.

^{99m}Tc-labeled Aβ probe designed via the conjugate strategy. These findings strongly suggest that [^{99m}Tc]**14b** should be evaluated in future studies.

Ex Vivo Autoradiography. The capability of [^{99m}Tc]**14b** to bind Aβ plaques in vivo was verified by ex vivo autoradiography in a Tg mouse and an age-matched wild-type mouse. Extensive labeling of Aβ plaques was observed in the cortical region of the Tg mouse, consistent with fluorescent staining by thioflavin-S (Figure 5). In the age-matched control mouse, no radioactive labeling or thioflavin-S-positive Aβ plaques were detected. These results demonstrate sufficient brain uptake and specific Aβ binding of [^{99m}Tc]**14b** in living mice.

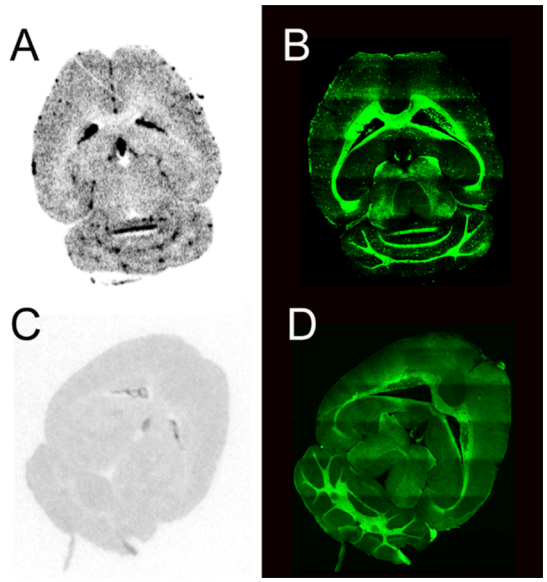

Figure 5. Ex vivo autoradiography of [^{99m}Tc]**14b** (A and C) in a Tg mouse (APPswe/PSEN1, male, 24 months old) and a wild-type mouse (C57BL6, male, 24 months old). The same brain slices were fluorescent stained with thioflavin-S (B and D).

DOI: 10.1021/acs.bioconjchem.6b00444
Bioconjugate Chem. XXXX, XXX, XXX−XXX

In Vivo SPECT−CT Imaging in Rhesus Monkeys. Experiments in mice verified the ability of [^{99m}Tc]**14b** to cross the BBB of rodents. Considering species differences, we assessed the ability of [^{99m}Tc]**14b** to cross the BBB of primates. In vivo SPECT and computed tomography (CT) imaging was conducted on two rhesus monkeys (M04: 4 years old, male; F27: 27 years old, female). The dynamic scan images revealed radioactivity accumulation in the brain, indicating permeation of [^{99m}Tc]**14b** through the BBB (Figure 6). The semi-

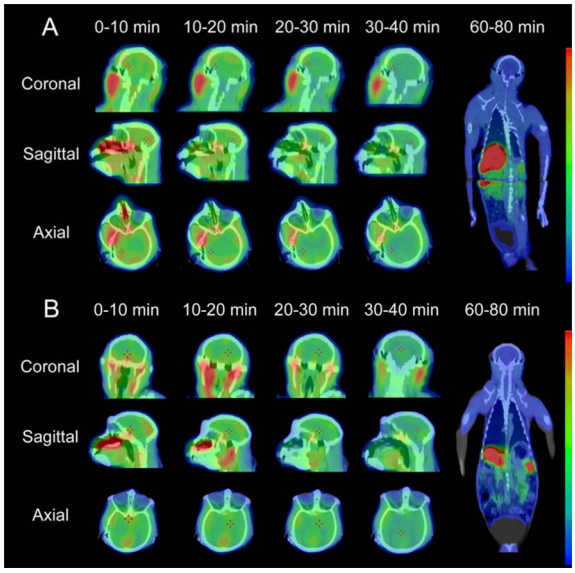

Figure 6. SPECT images of [^{99m}Tc]**14b** in rhesus monkeys (A: 4 years old, male; B: 27 years old, female); SPECT images are overlaid on individual co-registered CT images.

quantitative data showed brain uptakes peaked during 0−10 min post-injection with a reasonable clearance ratio (Table 3).

Table 3. Semi-Quantitative Brain Uptake of [^{99m}Tc]14b in Two Rhesus Monkeys[a]

	0−10 min	10−20 min	20−30 min	30−40 min	clearance ratio
M04	1.23	1.13	1.01	0.88	1.40
F27	0.78	0.70	0.67	0.64	1.22

[a]Expressed as percent injected dose.

There was obvious accumulation of radioactivity in some glands of the head, but this accumulation occurred outside of the brain. Whole-body scans were conducted to assess the distribution of radioactivity 60−80 min postinjection. Radioactivity accumulated mainly in the liver and kidneys, suggesting hepatobiliary and urinary elimination of the radiotracer.

Because we conducted only two cases of SPECT imaging in rhesus monkeys, no statistical analysis was performed. Absolute quantitation of tracer uptakes were not conducted due to the lack of quantitation module, which was not necessary for the hospital daily use. Nevertheless, this is the first assessment of a ^{99m}Tc-labeled Aβ probe in nonhuman primates; the results of this study highlight the usefulness of ^{99m}Tc-labeled Aβ probes.

CONCLUSIONS

We designed, synthesized, and characterized a series of 2-arylbenzothiazole derivatives for ^{99m}Tc labeling via conjugated approach. A total of seven compounds were screened via in vitro competitive binding assays, after which they were radiolabeled and biologically evaluated. In vitro fluorescent staining assays and in vitro autoradiography showed positive results. Among the seven ^{99m}Tc-labeled tracers, [^{99m}Tc]**14b** exhibited the most favorable brain pharmacokinetics in normal ICR mice. Ex vivo autoradiography using [^{99m}Tc]**14b** demonstrated sufficient brain uptake and specific Aβ binding in living Tg mice. Importantly, semiquantitative SPECT imaging showed [^{99m}Tc]**14b** penetrated the blood−brain barrier (BBB) of rhesus monkeys. [^{99m}Tc]**14b** is a promising SPECT imaging probe for Aβ plaques in AD brains that reveals the utility of ^{99m}Tc-labeled probes in this field.

EXPERIMENTAL SECTION

General. All chemicals used were purchased from commercial sources without further purification. Na^{99m}TcO$_4$ was eluted from a commercial ^{99}Mo−^{99m}Tc generator, which was obtained from Beijing Atomic High-Tech Co. Ltd. GH kits were purchased from Beijing ShiHong Pharmaceutical Center. NMR spectra were acquired on a Bruker Avance III spectrometer at room temperature with TMS as the internal standard. Chemical shifts are reported as δ values relative to TMS. Coupling constants are reported in Hz. Multiplicity is defined by s (singlet), d (doublet), t (triplet), and m (multiplet). Mass spectra were acquired with a Surveyor MSQ Plus (ESI) (Waltham, MA) instrument. HPLC purification and analysis were performed on a Shimadzu system (LC-20AD system with a Bioscan Flow Count 3200 NaI/PMT γ-radiation scintillation detector and a SPD-20AV UV detector, λ = 254 nm). Radioactivity was detected by an automatic γ-counter (WALLAC/Wizard 1470). Fluorescent staining was observed with an Axio Observer Z1 inverted fluorescence microscope (Zeiss, Germany) using a DAPI filter set (excitation, 405 nm). Monkey SPECT−CT scans were conducted on a Discovery NM/CT 670 system (GE Healthcare) at Xuanwu Hospital. Aβ_{1-42} peptides (trifluoroacetate form) were purchased from Peptide Institute, Inc. (Japan). Normal ICR mice (male, 5 weeks old) for the biodistribution studies were purchased from Vital River Co. Ltd. Transgenic mice (APPswe/PSEN1, male) and age-matched wild-type mice (C57BL6, male) were obtained from the Institute of Laboratory Animal Sciences, Chinese Academy of Medical Sciences. All protocols involving the use of animals were approved by the Animal Care Committee of Beijing Normal University and were also in accordance with ACS Ethical Guidelines. Human brain tissue from three autopsy-confirmed AD patients (64 years old, female; 91 years old, male; 68 years old, female) were obtained from the Chinese Brain Bank Center. Rhesus monkeys (4 years old, male; 27 years old, female) were provided by the Department of Laboratory Animal Sciences, School of Basic Medical Sciences, Capital Medical University.

Chemistry. Compounds **1**−**4** were prepared as reported previously.[33,34]

*General Synthesis Procedures for Compounds **5a**−**d**, **6a**−**d**, **7a**−**d**, and **8a**−**d**.* A mixture of **1**, **2**, **3**, or **4** (1.0 mmol); 1,3-dibromopropane, 1,4-dibromobutane, 1,5-dibromopentane, or 1,6-dibromohexane (2.0 mmol); and K_2CO_3 (3.0 mmol) in CH_3CN was heated to reflux with constant stirring for 2 h, after which it was filtered. Organic solvents were removed from the filtrate using rotary evaporation. Petroleum ether (10 mL) was added, after which the precipitate was filtered off, washed by

DOI: 10.1021/acs.bioconjchem.6b00444
Bioconjugate Chem. XXXX, XXX, XXX−XXX

petroleum ether, and collected for use in the next step of the synthesis.

*4-(6-(3-Bromopropoxy)benzo[d]thiazol-2-yl)-N,N-dimethylaniline (**5a**)*. Yield, 79%; mp 128.5−129.9 °C. ^{1}H NMR (400 MHz, $CDCl_3$, δ): 7.87 (d, J = 8.6 Hz, 2H), 7.86 (d, J = 8.9 Hz, 1H), 7.32 (d, J = 2.5 Hz, 1H), 7.03 (dd, J = 8.8, 2.5 Hz, 1H), 6.63 (d, J = 8.7 Hz, 2H), 4.16 (t, J = 5.8 Hz, 2H), 3.63 (t, J = 6.4 Hz, 2H), 2.89 (s, 6H), 2.31−2.39 (m, 2H).

*4-(6-(4-Bromobutoxy)benzo[d]thiazol-2-yl)-N,N-dimethylaniline (**5b**)*. Yield, 65%; mp 139.5−141.4 °C. ^{1}H NMR (400 MHz, $CDCl_3$, δ): 7.92 (d, J = 8.5 Hz, 2H), 7.87 (d, J = 8.8 Hz, 1H), 7.30 (d, J = 2.4 Hz, 1H), 7.02 (dd, J = 8.9, 2.5 Hz, 1H), 6.75 (d, J = 8.9 Hz, 2H), 4.06 (t, J = 6.0 Hz, 2H), 3.51 (t, J = 6.6 Hz, 2H), 3.06 (s, 6H), 2.07−2.15 (m, 2H), 1.95−2.03 (m, 2H).

*4-(6-((5-Bromopentyl)oxy)benzo[d]thiazol-2-yl)-N,N-dimethylaniline (**5c**)*. Yield, 45%; mp 185.1−186.3 °C. ^{1}H NMR (400 MHz, $CDCl_3$, δ): 7.92 (d, J = 8.8 Hz, 2H), 7.87 (d, J = 8.9 Hz, 1H), 7.30 (d, J = 2.4 Hz, 1H), 7.03 (dd, J = 8.9, 2.4 Hz, 1H), 6.75 (d, J = 8.8 Hz, 2H), 4.03 (t, J = 6.3 Hz, 2H), 3.45 (t, J = 6.8 Hz, 2H), 3.05 (s, 6H), 2.01−1.91 (m, 2H), 1.90−1.81 (m, 2H), 1.71−1.63 (m, 2H).

*4-(6-((6-Bromohexyl)oxy)benzo[d]thiazol-2-yl)-N,N-dimethylaniline (**5d**)*. Yield, 56%; mp 142.8−144.0 °C. ^{1}H NMR (400 MHz, $CDCl_3$, δ): 8.04−7.85 (m, 3H), 7.30 (d, J = 2.4 Hz, 1H), 7.04 (dd, J = 8.9, 2.2 Hz, 1H), 6.76 (d, J = 8.6 Hz, 2H), 4.03 (t, J = 6.4 Hz, 2H), 3.44 (t, J = 6.8 Hz, 2H), 3.06 (s, 6H), 1.96−1.88 (m, 2H), 1.88−1.79 (m, 2H), 1.57−1.50 (m, 4H).

*4-(6-(3-Bromopropoxy)benzo[d]thiazol-2-yl)-N-methylaniline (**6a**)*. Yield, 77%; mp 86.8−88.0 °C. ^{1}H NMR (400 MHz, $CDCl_3$, δ): 7.87 (d, J = 8.6 Hz, 2H), δ 7.86 (d, J = 8.8 Hz, 1H), δ 7.33 (d, J = 2.4 Hz, 1H), 7.04 (dd, J = 8.9, 2.5 Hz, 1H), 6.65 (d, J = 8.7 Hz, 2H), 4.17 (t, J = 5.8 Hz, 2H), 3.64 (t, J = 6.4 Hz, 2H), 2.91 (s, 3H), 2.32−2.40 (m, 2H).

*4-(6-(4-Bromobutoxy)benzo[d]thiazol-2-yl)-N-methylaniline (**6b**)*. Yield, 61%; mp 148.5−149.2 °C. ^{1}H NMR (400 MHz, $CDCl_3$, δ): 7.86 (d, J = 8.6 Hz, 2H), δ 7.85 (d, J = 8.7 Hz, 1H), δ 7.29 (d, J = 2.3 Hz, 1H), 7.02 (dd, J = 8.9, 2.4 Hz, 1H), 6.64 (d, J = 8.6 Hz, 2H), 4.05 (t, J = 6.0 Hz, 2H), 3.51 (t, J = 6.5 Hz, 2H), 2.90 (s, 3H), 2.12−2.05 (m, 2H), 2.02−1.93 (m, 2H).

*4-(6-((5-Bromopentyl)oxy)benzo[d]thiazol-2-yl)-N-methylaniline (**6c**)*. Yield, 78%; mp 114.9−115.6 °C. ^{1}H NMR (400 MHz, $CDCl_3$, δ): 7.89 (d, J = 8.6 Hz, 3H), 7.30 (d, J = 2.4 Hz, 1H), 7.03 (dd, J = 8.9, 2.6 Hz, 1H), 6.65 (d, J = 8.7 Hz, 2H), 4.03 (t, J = 6.3 Hz, 2H), 3.46 (t, J = 6.7 Hz, 2H), 2.91 (s, 3H), 2.00−1.92 (m, 2H), 1.90−1.81 (m, 2H), 1.70−1.63 (m, 2H).

*4-(6-((6-Bromohexyl)oxy)benzo[d]thiazol-2-yl)-N-methylaniline (**6d**)*. Yield, 65%; mp 125.3−126.5 °C. ^{1}H NMR (400 MHz, $CDCl_3$, δ): 7.87 (d, J = 8.5 Hz, 2H), δ 7.86 (d, J = 8.4 Hz, 1H), δ 7.30 (d, J = 2.3 Hz, 1H), 7.03 (dd, J = 8.9, 2.5 Hz, 1H), 6.64 (d, J = 8.6 Hz, 2H), 4.02 (t, J = 6.4 Hz, 2H), 3.44 (t, J = 6.8 Hz, 2H), 2.91 (s, 3H), 1.96−1.78 (m, 4H), 1.55−1.51 (m, 4H).

*5-(6-(3-Bromopropoxy)benzo[d]thiazol-2-yl)-N,N-dimethylpyridin-2-amine (**7a**)*. Yield, 89%; mp 128.8−131.8 °C. ^{1}H NMR (400 MHz, $CDCl_3$, δ): 8.76 (s, 1H), 8.15−8.11 (m, 1H), 7.87 (d, J = 8.7 Hz, 1H), 7.34 (s, 1H), 7.06 (t, J = 6.6 Hz, 1H), 6.58 (d, J = 9.0 Hz, 1H), 4.18 (t, J = 5.7 Hz, 2H), 3.64 (t, J = 6.4 Hz, 2H), 3.18 (s, 6H), 2.40−2.32 (m, 2H).

*5-(6-(4-Bromobutoxy)benzo[d]thiazol-2-yl)-N,N-dimethylpyridin-2-amine (**7b**)*. Yield, 68%; mp 124.2−125.0 °C. ^{1}H NMR (400 MHz, $CDCl_3$, δ): 8.76 (d, J = 2.0 Hz, 1H), 8.11 (dd, J = 9.0, 2.4 Hz, 1H), 7.86 (d, J = 8.9 Hz, 1H), 7.30 (d, J = 2.3 Hz, 1H), 7.03 (dd, J = 8.9, 2.4 Hz, 1H), 6.57 (d, J = 9.0 Hz, 1H), 4.05 (t, J = 6.0 Hz, 2H), 3.51 (t, J = 6.5 Hz, 2H), 3.17 (s, 6H), 2.14−2.04 (m, 2H), 2.02−1.93 (m, 2H).

*5-(6-((5-Bromopentyl)oxy)benzo[d]thiazol-2-yl)-N,N-dimethylpyridin-2-amine (**7c**)*. Yield, 85%; mp 144.5−145.5 °C. ^{1}H NMR (400 MHz, $CDCl_3$, δ): 8.76 (s, 1H), 8.14 (d, J = 8.9 Hz, 1H), 7.86 (d, J = 8.9 Hz, 1H), 7.31 (d, J = 1.9 Hz, 1H), 7.04 (dd, J = 8.9, 2.3 Hz, 1H), 6.60 (d, J = 9.0 Hz, 1H), 4.04 (t, J = 6.3 Hz, 2H), 3.46 (t, J = 6.7 Hz, 2H), 3.19 (s, 6H), 2.02−1.81 (m, 4H), 1.74−1.60 (m, 2H).

*5-(6-((6-Bromohexyl)oxy)benzo[d]thiazol-2-yl)-N,N-dimethylpyridin-2-amine (**7d**)*. Yield, 55%; mp 150.7−152.2 °C. ^{1}H NMR (400 MHz, $CDCl_3$, δ): 8.76 (d, J = 2.4 Hz, 1H), 8.16 (dd, J = 9.0, 2.2 Hz, 1H), 7.86 (d, J = 8.9 Hz, 1H), 7.31 (d, J = 2.4 Hz, 1H), 7.04 (dd, J = 8.9, 2.5 Hz, 1H), 6.60 (d, J = 9.0 Hz, 1H), 4.03 (t, J = 6.4 Hz, 2H), 3.44 (t, J = 6.8 Hz, 2H), 3.20 (s, 6H), 1.99−1.77 (m, 4H), 1.61−1.46 (m, 4H).

*5-(6-(3-Bromopropoxy)benzo[d]thiazol-2-yl)-N-methylpyridin-2-amine (**8a**)*. Yield, 83%; mp 122.2−123.5 °C. ^{1}H NMR (400 MHz, $CDCl_3$, δ): 8.72 (d, J = 2.0 Hz, 1H), 8.12 (dd, J = 8.8, 2.3 Hz, 1H), 7.88 (d, J = 8.9 Hz, 1H), 7.34 (d, J = 2.4 Hz, 1H), 7.06 (dd, J = 8.9, 2.5 Hz, 1H), 6.48 (d, J = 8.7 Hz, 1H), 5.01 (d, J = 4.6 Hz, 1H), 4.18 (t, J = 5.8 Hz, 2H), 3.64 (t, J = 6.4 Hz, 2H), 3.01 (d, J = 5.2 Hz, 3H), 2.36 (p, J = 6.1 Hz, 2H).

*5-(6-(4-Bromobutoxy)benzo[d]thiazol-2-yl)-N-methylpyridin-2-amine (**8b**)*. Yield, 55%; mp 152.9−154.6 °C. ^{1}H NMR (400 MHz, $CDCl_3$, δ): 8.72 (d, J = 1.9 Hz, 1H), 8.11 (dd, J = 8.7, 2.2 Hz, 1H), 7.86 (d, J = 8.9 Hz, 1H), 7.31 (d, J = 2.4 Hz, 1H), 7.04 (dd, J = 8.9, 2.4 Hz, 1H), 6.47 (d, J = 8.8 Hz, 1H), 4.99 (d, J = 4.4 Hz, 1H), 4.06 (t, J = 6.0 Hz, 2H), 3.51 (t, J = 6.5 Hz, 2H), 3.00 (d, J = 5.1 Hz, 3H), 2.17−2.05 (m, 2H), 2.04−1.94 (m, 2H).

*5-(6-((5-Bromopentyl)oxy)benzo[d]thiazol-2-yl)-N-methylpyridin-2-amine (**8c**)*. Yield, 73%; mp 124.7−125.6 °C. ^{1}H NMR (400 MHz, $CDCl_3$, δ): 8.72 (d, J = 1.9 Hz, 1H), 8.11 (dd, J = 8.7, 2.4 Hz, 1H), 7.87 (d, J = 8.9 Hz, 1H), 7.31 (d, J = 2.4 Hz, 1H), 7.04 (dd, J = 8.9, 2.5 Hz, 1H), 6.46 (d, J = 8.8 Hz, 1H), 4.94 (d, J = 4.9 Hz, 1H), 4.04 (t, J = 6.3 Hz, 2H), 3.46 (t, J = 6.7 Hz, 2H), 3.00 (d, J = 5.2 Hz, 3H), 2.01−1.92 (m, 2H), 1.90−1.82 (m, 2H), 1.69−1.63 (m, 2H).

*5-(6-((6-Bromohexyl)oxy)benzo[d]thiazol-2-yl)-N-methylpyridin-2-amine (**8d**)*. Yield, 63%; mp 116.4−117.6 °C. ^{1}H NMR (400 MHz, $CDCl_3$, δ): 8.72 (d, J = 2.4 Hz, 1H), 8.11 (dd, J = 8.7, 2.4 Hz, 1H), 7.86 (d, J = 8.9 Hz, 1H), 7.31 (d, J = 2.5 Hz, 1H), 7.04 (dd, J = 8.9, 2.5 Hz, 1H), 6.46 (d, J = 8.8 Hz, 1H), 4.94 (d, J = 4.9 Hz, 1H), 4.02 (t, J = 6.4 Hz, 2H), 3.44 (t, J = 6.8 Hz, 2H), 3.00 (d, J = 5.2 Hz, 3H), 1.97−1.78 (m, 4H), 1.57−1.50 (m, 4H).

*General Synthesis Procedures for Precursors **9a−d, 10a−d, 11a−d, and 12a−d***. A mixture of **5a−d**, **6a−d**, **7a−d**, or **8a−d** (0.30 mmol); BAT−Boc (0.25 mmol), K_2CO_3 (0.50 mmol), and KI (0.25 mmol) in CH_3CN was heated to reflux with constant stirring for 24 h, after which it was filtered. The filtrate was concentrated under reduced pressure. Purification by column chromatography (petroleum ether−ethyl acetate, 4:1) produced a white spumescent solid.

*Tert-butyl(2-((3-((2-(4-(dimethylamino)phenyl)benzo[d]thiazol-6-yl)oxy)propyl)(2-(tritylthio)ethyl)amino)ethyl)(2-(tritylthio)ethyl)carbamate (**9a**)*. Yield, 28%; mp 49.7−51.1 °C. ^{1}H NMR (400 MHz, $CDCl_3$, δ): 7.90 (d, J = 8.9 Hz, 2H), 7.81 (d, J = 8.9 Hz, 1H), 7.43−7.34 (m, 13H), 7.28−7.14 (m, 18H), 6.95 (d, J = 8.7 Hz, 1H), 6.75 (d, J = 8.9 Hz, 2H), 3.93

DOI: 10.1021/acs.bioconjchem.6b00444
Bioconjugate Chem. XXXX, XXX, XXX−XXX

(t, J = 6.1 Hz, 2H), 3.05 (s, 6H), 3.00−2.77 (m, 4H), 2.44−2.20 (m, 10H), 1.78−1.66 (m, 2H), 1.36 (s, 9H). MS (ESI) m/z: $[M + H]^+$ calcd for $C_{67}H_{71}N_4O_3S_3$, 1075.5; found, 1075.2.

*Tert-butyl(2-((4-((2-(4-(dimethylamino)phenyl)benzo[d]-thiazol-6-yl)oxy)butyl)(2-(tritylthio)ethyl)amino)ethyl)(2-(tritylthio)ethyl)carbamate (**9b**).* Yield, 29%; mp 58.6−60.0 °C. ^{1}H NMR (400 MHz, $CDCl_3$, δ): 7.90 (d, J = 8.8 Hz, 2H), 7.84 (d, J = 8.9 Hz, 1H), 7.40 (d, J = 7.6 Hz, 13H), 7.31−7.22 (m, 12H), 7.21−7.13 (m, 6H), 6.99 (dd, J = 8.8, 2.1 Hz, 1H), 6.73 (d, J = 8.9 Hz, 2H), 3.93 (t, J = 6.2 Hz, 2H), 3.03 (s, 6H), 3.00−2.79 (m, 4H), 2.41−2.16 (m, 10H), 1.76−1.63 (m, 2H), 1.48−1.30 (m, 11H). MS (ESI) m/z: $[M + H]^+$ calcd for $C_{68}H_{73}N_4O_3S_3$, 1089.5; found, 1089.2.

*Tert-butyl (2-((5-((2-(4-(dimethylamino)phenyl)benzo[d]-thiazol-6-yl)oxy)pentyl)(2-(tritylthio)ethyl)amino)ethyl)(2-(tritylthio)ethyl)carbamate (**9c**).* Yield, 43%; mp 49.9−51.3 °C. ^{1}H NMR (400 MHz, $CDCl_3$, δ): 7.90 (d, J = 8.9 Hz, 2H), 7.84 (d, J = 8.9 Hz, 1H), 7.45−7.34 (m, 12H), 7.32−7.22 (m, 13H), 7.22−7.14 (m, 6H), 7.00 (d, J = 6.9 Hz, 1H), 6.74 (d, J = 8.9 Hz, 2H), 3.96 (t, J = 6.2 Hz, 2H), 3.05 (s, 6H), 3.01−2.82 (m, 4H), 2.42−2.14 (m, 8H), 1.80−1.70 (m, 2H), 1.61−1.51 (m, 2H), 1.44−1.28 (m, 13H). MS (ESI) m/z: $[M + H]^+$ calcd for $C_{69}H_{75}N_4O_3S_3$, 1103.5; found, 1103.1.

*Tert-butyl (2-((6-((2-(4-(dimethylamino)phenyl)benzo[d]-thiazol-6-yl)oxy)hexyl)(2-(tritylthio)ethyl)amino)ethyl)(2-(tritylthio)ethyl)carbamate (**9d**).* Yield, 37%; mp 52.3−53.4 °C. ^{1}H NMR (400 MHz, $CDCl_3$, δ): 7.90 (d, J = 8.9 Hz, 2H), 7.84 (d, J = 8.9 Hz, 1H), 7.45−7.35 (m, 12H), 7.32−7.22 (m, 13H), 7.22−7.13 (m, 6H), 7.01 (dd, J = 8.9, 2.4 Hz, 1H), 6.74 (d, J = 9.0 Hz, 2H), 3.98 (t, J = 6.4 Hz, 2H), 3.05 (s, 6H), 3.00−2.78 (m, 4H), 2.40−2.14 (m, 8H), 1.84−1.72 (m, 2H), 1.47−1.31 (m, 13H), 1.30−1.18 (m, 4H). MS (ESI) m/z: $[M + H]^+$ calcd for $C_{70}H_{77}N_4O_3S_3$, 1117.5; found, 1117.1.

*Tert-butyl (2-((3-((2-(4-(methylamino)phenyl)benzo[d]-thiazol-6-yl)oxy)propyl)(2-(tritylthio)ethyl)amino)ethyl)(2-(tritylthio)ethyl)carbamate (**10a**).* Yield, 24%; mp 57.2−58.5 °C. ^{1}H NMR (400 MHz, $CDCl_3$, δ): 7.87 (d, J = 8.6 Hz, 2H), 7.81 (d, J = 8.9 Hz, 1H), 7.42−7.35 (m, 12H), 7.30−7.13 (m, 19H), 6.95 (d, J = 7.1 Hz, 1H), 6.65 (d, J = 8.7 Hz, 2H), 3.93 (t, J = 6.1 Hz, 2H), 3.06−2.80 (m, 7H), 2.44−2.19 (m, 10H), 1.76−1.69 (m, 2H), 1.42−1.33 (m, 9H). MS (ESI) m/z: $[M + H]^+$ calcd for $C_{66}H_{69}N_4O_3S_3$, 1061.5; found, 1060.9.

*Tert-butyl (2-((4-((2-(4-(methylamino)phenyl)benzo[d]-thiazol-6-yl)oxy)butyl)(2-(tritylthio)ethyl)amino)ethyl)(2-(tritylthio)ethyl)carbamate (**10b**).* Yield, 28%; mp 55.1−56.5 °C. ^{1}H NMR (400 MHz, $CDCl_3$, δ): 7.94−7.81 (m, 3H), 7.50−7.35 (m, 12H), 7.35−7.16 (m, 19H), 7.01 (dd, J = 8.9, 2.3 Hz, 1H), 6.64 (d, J = 8.7 Hz, 2H), 3.95 (t, J = 6.1 Hz, 2H), 3.12−2.78 (m, 7H), 2.49−2.16 (m, 10H), 1.77−1.65 (m, 2H), 1.50−1.33 (m, 11H). MS (ESI) m/z: $[M + H]^+$ calcd for $C_{67}H_{71}N_4O_3S_3$, 1075.5; found, 1075.1.

*Tert-butyl (2-((5-((2-(4-(methylamino)phenyl)benzo[d]-thiazol-6-yl)oxy)pentyl)(2-(tritylthio)ethyl)amino)ethyl)(2-(tritylthio)ethyl)carbamate (**10c**).* Yield, 59%; mp 53.7−54.9 °C. ^{1}H NMR (400 MHz, $CDCl_3$, δ): 7.87 (d, J = 8.7 Hz, 2H), 7.84 (d, J = 8.9 Hz, 1H), 7.44−7.36 (m, 12H), 7.32−7.22 (m, 13H), 7.22−7.13 (m, 6H), 7.01 (dd, J = 8.9, 2.5 Hz, 1H), 6.64 (d, J = 8.7 Hz, 2H), 3.96 (t, J = 6.4 Hz, 2H), 3.09−2.79 (m, 7H), 2.43−2.13 (m, 10H), 1.80−1.70 (m, 2H), 1.44−1.28 (m, 13H). MS (ESI) m/z: $[M + H]^+$ calcd for $C_{68}H_{73}N_4O_3S_3$, 1089.5; found, 1089.1.

*Tert-butyl (2-((6-((2-(4-(methylamino)phenyl)benzo[d]-thiazol-6-yl)oxy)hexyl)(2-(tritylthio)ethyl)amino)ethyl)(2-(tritylthio)ethyl)carbamate (**10d**).* Yield, 51%; mp 53.4−54.6 °C. ^{1}H NMR (400 MHz, $CDCl_3$, δ): 7.90−7.82 (m, 3H), 7.44−7.36 (m, 12H), 7.32−7.22 (m, 13H), 7.22−7.14 (m, 6H), 7.01 (dd, J = 8.9, 2.5 Hz, 1H), 6.64 (d, J = 8.7 Hz, 2H), 3.98 (t, J = 6.4 Hz, 2H), 3.09−2.78 (m, 7H), 2.41−2.11 (m, 10H), 1.83−1.73 (m, 2H), 1.47−1.32 (m, 11H), 1.30−1.20 (m, 4H). MS (ESI) m/z: $[M + H]^+$ calcd for $C_{69}H_{75}N_4O_3S_3$, 1103.5; found, 1103.2.

*Tert-butyl (2-((3-((2-(6-(dimethylamino)pyridin-3-yl)-benzo[d]thiazol-6-yl)oxy)propyl)(2-(tritylthio)ethyl)amino)-ethyl)(2-(tritylthio)ethyl)carbamate (**11a**).* Yield, 18%; mp 49.1−50.3 °C. ^{1}H NMR (400 MHz, $CDCl_3$, δ): 8.76 (d, J = 2.3 Hz, 1H), 8.12 (dd, J = 9.0, 2.4 Hz, 1H), 7.82 (d, J = 8.9 Hz, 1H), 7.43−7.35 (m, 12H), 7.29−7.12 (m, 19H), 6.97 (dd, J = 8.8, 2.0 Hz, 1H), 6.57 (d, J = 9.0 Hz, 1H), 3.94 (t, J = 6.1 Hz, 2H), 3.16 (s, 6H), 3.06−2.81 (m, 4H), 2.42−2.20 (m, 10H), 1.76−1.69 (m, 2H), 1.37 (s, 9H). MS (ESI) m/z: $[M + H]^+$ calcd for $C_{66}H_{70}N_5O_3S_3$, 1075.5; found, 1075.8.

*Tert-butyl (2-((4-((2-(6-(dimethylamino)pyridin-3-yl)-benzo[d]thiazol-6-yl)oxy)butyl)(2-(tritylthio)ethyl)amino)-ethyl)(2-(tritylthio)ethyl)carbamate (**11b**).* Yield, 32%; mp 52.8−53.9 °C. ^{1}H NMR (400 MHz, $CDCl_3$, δ): 8.76 (d, J = 2.2 Hz, 1H), 8.12 (dd, J = 9.0, 2.3 Hz, 1H), 7.84 (d, J = 8.9 Hz, 1H), 7.45−7.34 (m, 12H), 7.32−7.22 (m, 13H), 7.21−7.13 (m, 6H), 7.01 (dd, J = 8.9, 2.3 Hz, 1H), 6.56 (d, J = 9.0 Hz, 1H), 3.94 (t, J = 6.3 Hz, 2H), 3.15 (s, 6H), 3.07−2.81 (m, 4H), 2.42−2.18 (m, 10H), 1.76−1.65 (m, 2H), 1.50−1.31 (m, 11H). MS (ESI) m/z: $[M + H]^+$ calcd for $C_{67}H_{72}N_5O_3S_3$, 1090.5; found, 1090.1.

*Tert-butyl (2-((5-((2-(6-(dimethylamino)pyridin-3-yl)-benzo[d]thiazol-6-yl)oxy)pentyl)(2-(tritylthio)ethyl)amino)-ethyl)(2-(tritylthio)ethyl)carbamate (**11c**).* Yield, 26%; mp 37.2−38.3 °C. ^{1}H NMR (400 MHz, $CDCl_3$, δ): 8.76 (d, J = 2.3 Hz, 1H), 8.13 (dd, J = 9.0, 2.4 Hz, 1H), 7.85 (d, J = 8.9 Hz, 1H), 7.44−7.36 (m, 12H), 7.32−7.22 (m, 13H), 7.22−7.14 (m, 6H), 7.02 (dd, J = 8.9, 2.4 Hz, 1H), 6.58 (d, J = 9.0 Hz, 1H), 3.97 (t, J = 6.5 Hz, 2H), 3.18 (s, 6H), 3.08−2.81 (m, 4H), 2.40−2.16 (m, 10H), 1.80−1.71 (m, 2H), 1.47−1.28 (m, 13H). MS (ESI) m/z: $[M + H]^+$ calcd for $C_{68}H_{74}N_5O_3S_3$, 1104.5; found, 1103.8.

*Tert-butyl (2-((6-((2-(6-(dimethylamino)pyridin-3-yl)-benzo[d]thiazol-6-yl)oxy)hexyl)(2-(tritylthio)ethyl)amino)-ethyl)(2-(tritylthio)ethyl)carbamate (**11d**).* Yield, 64%; mp 48.5−49.4 °C. ^{1}H NMR (400 MHz, $CDCl_3$, δ): 8.76 (d, J = 2.3 Hz, 1H), 8.13 (dd, J = 9.0, 2.5 Hz, 1H), 7.85 (d, J = 8.9 Hz, 1H), 7.45−7.35 (m, 12H), 7.31−7.23 (m, 13H), 7.22−7.13 (m, 6H), 7.03 (dd, J = 8.9, 2.5 Hz, 1H), 6.58 (d, J = 9.0 Hz, 1H), 3.98 (t, J = 6.4 Hz, 2H), 3.18 (s, 6H), 3.08−2.78 (m, 4H), 2.39−2.12 (m, 10H), 1.83−1.74 (m, 2H), 1.47−1.34 (m, 11H), 1.29−1.22 (m, 4H). MS (ESI) m/z: $[M + H]^+$ calcd for $C_{69}H_{76}N_5O_3S_3$, 1118.5; found, 1118.2.

*Tert-butyl (2-((3-((2-(6-(methylamino)pyridin-3-yl)benzo-[d]thiazol-6-yl)oxy)propyl)(2-(tritylthio)ethyl)amino)ethyl)(2-(tritylthio)ethyl)carbamate (**12a**).* Yield, 49%; mp 58.9−59.9 °C. ^{1}H NMR (400 MHz, $CDCl_3$, δ): 8.71 (d, J = 1.8 Hz, 1H), 8.13 (dd, J = 8.8, 2.2 Hz, 1H), 7.83 (d, J = 8.9 Hz, 1H), 7.44−7.35 (m, 12H), 7.30−7.21 (m, 13H), 7.21−7.14 (m, 6H), 6.97 (d, J = 9.2 Hz, 1H), 6.48 (d, J = 8.8 Hz, 1H), 5.02 (s, 1H), 3.94 (t, J = 6.0 Hz, 2H), 3.06−2.83 (m, 7H), 2.45−2.20 (m, 8H), 1.79−1.69 (m, 2H), 1.67−1.56 (m, 2H), 1.37 (s, 9H). MS (ESI) m/z: $[M + H]^+$ calcd for $C_{65}H_{67}N_5O_3S_3$, 1062.4; found, 1062.4.

DOI: 10.1021/acs.bioconjchem.6b00444
Bioconjugate Chem. XXXX, XXX, XXX−XXX

*Tert-butyl (2-((4-((2-(6-(methylamino)pyridin-3-yl)benzo[d]thiazol-6-yl)oxy)butyl)(2-(tritylthio)ethyl)amino)ethyl)(2-(tritylthio)ethyl)carbamate (**12b**).* Yield, 46%; mp 51.7−53.1 °C. ^{1}H NMR (400 MHz, $CDCl_3$, δ): 8.73 (d, J = 2.0 Hz, 1H), 8.11 (dd, J = 8.8, 2.2 Hz, 1H), 7.87 (d, J = 8.9 Hz, 1H), 7.47−7.36 (m, 12H), 7.32−7.23 (m, 13H), 7.23−7.14 (m, 6H), 7.02 (dd, J = 8.9, 2.4 Hz, 1H), 6.47 (d, J = 8.8 Hz, 1H), 5.04 (d, J = 4.7 Hz, 1H), 3.95 (t, J = 6.3 Hz, 2H), 3.09−2.81 (m, 7H), 2.41−2.20 (m, 10H), 1.76−1.66 (m, 2H), 1.49−1.31 (m, 11H). MS (ESI) m/z: $[M + H]^+$ calcd for $C_{66}H_{70}N_5O_3S_3$, 1076.5; found, 1076.1.

*Tert-butyl (2-((5-((2-(6-(methylamino)pyridin-3-yl)benzo[d]thiazol-6-yl)oxy)pentyl)(2-(tritylthio)ethyl)amino)ethyl)(2-(tritylthio)ethyl)carbamate (**12c**).* Yield, 44%; mp 52.6−54.0 °C. ^{1}H NMR (400 MHz, $CDCl_3$, δ): 8.72 (d, J = 2.1 Hz, 1H), 8.12 (dd, J = 8.8, 2.4 Hz, 1H), 7.86 (d, J = 8.9 Hz, 1H), 7.44−7.34 (m, 12H), 7.31−7.22 (m, 13H), 7.22−7.14 (m, 6H), 7.03 (dd, J = 8.9, 2.5 Hz, 1H), 6.47 (d, J = 8.8 Hz, 1H), 4.91 (d, J = 4.7 Hz, 1H), 3.97 (t, J = 6.4 Hz, 2H), 3.09−2.79 (m, 7H), 2.41−2.12 (m, 10H), 1.81−1.70 (m, 2H), 1.44−1.29 (m, 13H). MS (ESI) m/z: $[M + H]^+$ calcd for $C_{67}H_{72}N_5O_3S_3$, 1090.5; found, 1090.2.

*Tert-butyl (2-((6-((2-(6-(methylamino)pyridin-3-yl)benzo[d]thiazol-6-yl)oxy)hexyl)(2-(tritylthio)ethyl)amino)ethyl)(2-(tritylthio)ethyl)carbamate (**12d**).* Yield, 51%; mp 40.6−41.5 °C. ^{1}H NMR (400 MHz, $CDCl_3$, δ): 8.70 (d, J = 2.1 Hz, 1H), 8.14 (dd, J = 8.8, 2.4 Hz, 1H), 7.86 (d, J = 8.9 Hz, 1H), 7.46−7.36 (m, 12H), 7.31−7.23 (m, 13H), 7.22−7.15 (m, 6H), 7.04 (dd, J = 8.9, 2.5 Hz, 1H), 6.49 (d, J = 8.8 Hz, 1H), 5.22 (s, 1H), 3.98 (t, J = 6.4 Hz, 2H), 3.16−2.79 (m, 7H), 2.46−2.10 (m, 10H), 1.83−1.73 (m, 2H), 1.48−1.33 (m, 11H), 1.30−1.21 (m, 4H). MS (ESI) m/z: $[M + H]^+$ calcd for $C_{68}H_{74}N_5O_3S_3$, 1104.5; found, 1104.2.

*General Synthesis Procedures for Rhenium Complexes **13a−d**, **14a−d**, **15a−d**, and **16a−d**.* The corresponding precursor (0.05 mmol) was dissolved in trifluoroacetic acid (2 mL) and stirred at 0 °C for 10 min. After triethyl silicane (40 μL) was added, the mixture was stirred at 0 °C for 10 min. Trifluoroacetic acid was removed under reduced pressure. The residue was dissolved in a mixed solvent (CH_2Cl_2−MeOH, 9:1, 20 mL), after which $(PPh_3)_2ReOCl_3$ (41.7 mg, 0.05 mmol) and anhydrous sodium acetate (20.0 mg) were added. The mixture was heated to reflux under constant stirring for 2 h and concentrated by rotary evaporation. Purification by column chromatography (CH_2Cl_2−MeOH, 200:1) produced a pink solid. HPLC purity analysis conditions: Waters 5C18-AR 300 column (5 μm, 4.6 × 150 mm); eluent A, H_2O; eluent B, CH_3CN; B%, 70% for **13a−d** and **15a−d**, 60% for **14a−d** and **16a−d**; flow rate, 1 mL/min; detection wavelength, 254 nm; column temperature, rt.

*2-((3-((2-(4-(Dimethylamino)phenyl)benzo[d]thiazol-6-yl)oxy)propyl)(2-((2-mercaptoethyl)amino)ethyl)amino)ethane-1-thiol-rhenium(V) oxide (**13a**).* Yield, 47%; mp 239.5−240.3 °C. ^{1}H NMR (400 MHz, DMSO-d_6, δ): 7.88−7.79 (m, 3H), 7.67 (d, J = 2.5 Hz, 1H), 7.10 (dd, J = 8.9, 2.5 Hz, 1H), 6.81 (d, J = 9.0 Hz, 2H), 4.21−4.04 (m, 5H), 3.90−3.78 (m, 1H), 3.67−3.49 (m, 3H), 3.46−3.35 (m, 1H), 3.32−3.16 (m, 2H), 3.10−3.03 (m, 1H), 3.01 (s, 6H), 2.74−2.62 (m, 2H), 2.36−2.23 (m, 2H), 1.75−1.65 (m, 1H). HRMS (ESI) m/z: $[M + H]^+$ calcd for $C_{24}H_{32}N_4O_2S_3{}^{187}Re$, 691.1245; found, 691.1242. HPLC retention time: 7.30 min, 96.5%.

*2-((4-((2-(4-(Dimethylamino)phenyl)benzo[d]thiazol-6-yl)oxy)butyl)(2-((2-mercaptoethyl)amino)ethyl)amino)ethane-1-thiol-rhenium(V) oxide (**13b**).* Yield, 66%; mp 228.7−229.7 °C. ^{1}H NMR (400 MHz, $CDCl_3$, δ): 7.91 (d, J = 8.8 Hz, 2H), 7.87 (d, J = 9.0 Hz, 1H), 7.32 (d, J = 2.4 Hz, 1H), 7.03 (dd, J = 8.9, 2.4 Hz, 1H), 6.74 (d, J = 8.9 Hz, 2H), 4.25−4.05 (m, 5H), 3.94−3.84 (m, 1H), 3.83−3.73 (m, 1H), 3.69−3.58 (m, 1H), 3.48−3.31 (m, 3H), 3.31−3.21 (m, 1H), 3.05 (s, 6H), 3.03−2.94 (m, 2H), 2.79−2.70 (m, 1H), 2.10−1.99 (m, 2H), 1.93−1.83 (m, 2H), 1.77−1.66 (m, 1H). HRMS (ESI) m/z: $[M + H]^+$ calcd for $C_{25}H_{34}N_4O_2S_3{}^{185}Re$, 703.1374; found, 703.1361. HPLC retention time: 8.93 min, 97.8%.

*2-((5-((2-(4-(Dimethylamino)phenyl)benzo[d]thiazol-6-yl)oxy)pentyl)(2-((2-mercaptoethyl)amino)ethyl)amino)ethane-1-thiol-rhenium(V) oxide (**13c**).* Yield, 53%; mp 229.9−231.0 °C. ^{1}H NMR (400 MHz, $CDCl_3$, δ): 7.99−7.86 (m, 3H), 7.31 (d, J = 2.2 Hz, 1H), 7.03 (dd, J = 8.9, 2.2 Hz, 1H), 6.76 (d, J = 8.6 Hz, 2H), 4.18−4.09 (m, 3H), 4.06 (t, J = 6.0 Hz, 2H), 3.91−3.82 (m, 1H), 3.82−3.75 (m, 1H), 3.64−3.54 (m, 1H), 3.43−3.31 (m, 3H), 3.30−3.20 (m, 1H), 3.06 (s, 6H), 3.04−2.94 (m, 2H), 2.79−2.70 (m, 1H), 1.97−1.84 (m, 4H), 1.77−1.69 (m, 1H), 1.64−1.58 (m, 2H). HRMS (ESI) m/z: $[M + H]^+$ calcd for $C_{26}H_{36}N_4O_2S_3{}^{187}Re$, 719.1558; found: 719.1569. HPLC retention time: 12.08 min, 97.8%.

*2-((6-((2-(4-(Dimethylamino)phenyl)benzo[d]thiazol-6-yl)oxy)hexyl)(2-((2-mercaptoethyl)amino)ethyl)amino)ethane-1-thiol-rhenium(V) oxide (**13d**).* Yield, 29%; mp 211.8−213.1 °C. ^{1}H NMR (400 MHz, $CDCl_3$, δ): 7.91 (d, J = 8.9 Hz, 2H), 7.87 (d, J = 8.9 Hz, 1H), 7.31 (d, J = 2.4 Hz, 1H), 7.03 (dd, J = 8.9, 2.5 Hz, 1H), 6.75 (d, J = 8.9 Hz, 2H), 4.16−4.08 (m, 3H), 4.04 (t, J = 6.2 Hz, 2H), 3.88−3.74 (m, 2H), 3.60−3.50 (m, 1H), 3.40−3.30 (m, 3H), 3.29−3.19 (m, 1H), 3.05 (s, 6H), 3.03−2.93 (m, 2H), 2.77−2.69 (m, 1H), 1.90−1.77 (m, 4H), 1.74−1.66 (m, 1H), 1.62−1.57 (m, 2H), 1.51−1.44 (m, 2H). HRMS (ESI) m/z: $[M + H]^+$ calcd for $C_{27}H_{38}N_4O_2S_3{}^{185}Re$, 731.1687; found, 731.1699. HPLC retention time: 15.32 min, 98.8%.

*2-((2-((2-Mercaptoethyl)(3-((2-(4-(methylamino)phenyl)benzo[d]thiazol-6-yl)oxy)propyl)amino)ethyl)amino)ethane-1-thiol-rhenium(V) oxide (**14a**).* Yield, 28%; mp 179.8−181.5 °C. ^{1}H NMR (400 MHz, DMSO-d_6, δ): 7.80 (d, J = 8.9 Hz, 1H), 7.76 (d, J = 8.7 Hz, 2H), 7.65 (d, J = 2.5 Hz, 1H), 7.08 (dd, J = 8.8, 2.4 Hz, 1H), 6.64 (d, J = 8.7 Hz, 2H), 5.75 (s, 1H), 4.16 (t, J = 6.1 Hz, 2H), 4.14−4.03 (m, 3H), 3.88−3.79 (m, 1H), 3.65−3.50 (m, 3H), 3.44−3.35 (m, 1H), 3.29−3.17 (m, 2H), 3.06 (d, J = 11.1 Hz, 1H), 2.75 (d, J = 4.9 Hz, 3H), 2.71−2.64 (m, 2H), 2.35−2.24 (m, 2H), 1.76−1.66 (m, 1H). HRMS (ESI) m/z: $[M + H]^+$ calcd for $C_{23}H_{30}N_4O_2S_3{}^{187}Re$, 677.1089; found, 677.1080. HPLC retention time: 8.12 min, 99.5%.

*2-((2-((2-Mercaptoethyl)(4-((2-(4-(methylamino)phenyl)benzo[d]thiazol-6-yl)oxy)butyl)amino)ethyl)amino)ethane-1-thiol-rhenium(V) oxide (**14b**).* Yield, 30%; mp 120.4−121.6 °C. ^{1}H NMR (400 MHz, $CDCl_3$, δ): 8.01−7.83 (m, 3H), 7.32 (d, J = 2.3 Hz, 1H), 7.06 (d, J = 8.9 Hz, 1H), 6.66 (d, J = 8.6 Hz, 2H), 4.24−4.06 (m, 5H), 3.95−3.86 (m, 1H), 3.83−3.76 (m, 1H), 3.70−3.59 (m, 1H), 3.49−3.32 (m, 3H), 3.32−3.22 (m, 1H), 3.07−2.97 (m, 2H), 2.92 (s, 3H), 2.79−2.71 (m, 1H), 2.12−1.99 (m, 2H), 1.94−1.86 (m, 2H), 1.77−1.68 (m, 1H). HRMS (ESI) m/z: $[M + H]^+$ calcd for $C_{24}H_{32}N_4O_2S_3{}^{185}Re$, 689.1217; found, 689.1224. HPLC retention time: 10.11 min, 96.9%.

*2-((2-((2-Mercaptoethyl)(5-((2-(4-(methylamino)phenyl)benzo[d]thiazol-6-yl)oxy)pentyl)amino)ethyl)amino)ethane-1-thiol-rhenium(V) oxide (**14c**).* Yield, 37%; mp 187.2−188.6 °C. ^{1}H NMR (400 MHz, $CDCl_3$, δ): 7.92−7.83 (m, 3H), 7.31

DOI: 10.1021/acs.bioconjchem.6b00444
Bioconjugate Chem. XXXX, XXX, XXX−XXX

(d, J = 2.5 Hz, 1H), 7.02 (dd, J = 8.9, 2.5 Hz, 1H), 6.65 (d, J = 8.7 Hz, 2H), 4.17−4.09 (m, 3H), 4.05 (t, J = 6.1 Hz, 2H), 3.91−3.82 (m, 1H), 3.82−3.75 (m, 1H), 3.63−3.53 (m, 1H), 3.43−3.31 (m, 3H), 3.29−3.21 (m, 1H), 3.06−2.94 (m, 2H), 2.91 (s, 3H), 2.79−2.71 (m, 1H), 1.96−1.83 (m, 4H), 1.76−1.67 (m, 1H), 1.64−1.55 (m, 2H). HRMS (ESI) m/z: $[M + H]^+$ calcd for $C_{25}H_{34}N_4O_2S_3{}^{185}Re$, 703.1374; found, 703.1384. HPLC retention time: 13.74 min, 99.1%.

*2-((2-((2-Mercaptoethyl)(6-((2-(4-(methylamino)phenyl)benzo[d]thiazol-6-yl)oxy)hexyl)amino)ethyl)amino)ethane-1-thiol-rhenium(V) oxide (**14d**).* Yield, 61%; mp 111.1−112.3 °C. ^{1}H NMR (400 MHz, $CDCl_3$, δ): 7.92−7.83 (m, 3H), 7.31 (d, J = 2.4 Hz, 1H), 7.03 (dd, J = 8.9, 2.5 Hz, 1H), 6.65 (d, J = 8.7 Hz, 2H), 4.16−4.07 (m, 3H), 4.04 (t, J = 6.2 Hz, 2H), 3.89−3.74 (m, 2H), 3.59−3.49 (m, 1H), 3.42−3.30 (m, 3H), 3.28−3.19 (m, 1H), 3.05−2.93 (m, 2H), 2.91 (s, 3H), 2.77−2.69 (m, 1H), 1.89−1.77 (m, 4H), 1.74−1.65 (m, 1H), 1.64−1.55 (m, 2H), 1.50−1.41 (m, 2H). HRMS (ESI) m/z: $[M + H]^+$ calcd for $C_{26}H_{36}N_4O_2S_3{}^{185}Re$, 717.1530; found, 717.1518. HPLC retention time: 19.27 min, 98.5%.

*2-((3-((2-(6-(Dimethylamino)pyridin-3-yl)benzo[d]thiazol-6-yl)oxy)propyl)(2-((2-mercaptoethyl)amino)ethyl)amino)-ethane-1-thiol-rhenium(V) oxide (**15a**).* Yield, 53%; mp 236.4−237.9 °C. ^{1}H NMR (400 MHz, DMSO-d_6, δ): 8.71 (d, J = 2.4 Hz, 1H), 8.09 (dd, J = 9.0, 2.5 Hz, 1H), 7.86 (d, J = 8.9 Hz, 1H), 7.70 (d, J = 2.5 Hz, 1H), 7.12 (dd, J = 8.9, 2.5 Hz, 1H), 6.80 (d, J = 9.1 Hz, 1H), 4.17 (t, J = 6.2 Hz, 2H), 4.15−4.04 (m, 3H), 3.89−3.79 (m, 1H), 3.65−3.51 (m, 5H), 3.30−3.18 (m, 2H), 3.13 (s, 6H), 2.75−2.63 (m, 2H), 2.35−2.24 (m, 2H), 1.76−1.66 (m, 1H). HRMS (ESI) m/z: $[M + H]^+$ calcd for $C_{23}H_{31}N_5O_2S_3{}^{187}Re$, 692.1198; found, 692.1194. HPLC retention time: 5.18 min, 98.7%.

*2-((4-((2-(6-(Dimethylamino)pyridin-3-yl)benzo[d]thiazol-6-yl)oxy)butyl)(2-((2-mercaptoethyl)amino)ethyl)amino)-ethane-1-thiol-rhenium(V) oxide (**15b**).* Yield, 44%; mp 231.2−231.9 °C. ^{1}H NMR (400 MHz, $CDCl_3$, δ): 8.76 (d, J = 2.1 Hz, 1H), 8.14 (d, J = 7.4 Hz, 1H), 7.88 (d, J = 8.9 Hz, 1H), 7.33 (d, J = 2.4 Hz, 1H), 7.05 (dd, J = 8.9, 2.4 Hz, 1H), 6.60 (d, J = 8.3 Hz, 1H), 4.26−4.06 (m, 5H), 3.96−3.85 (m, 1H), 3.83−3.75 (m, 1H), 3.71−3.59 (m, 1H), 3.51−3.33 (m, 3H), 3.31−3.24 (m, 1H), 3.19 (s, 6H), 3.07−2.96 (m, 2H), 2.80−2.71 (m, 1H), 2.12−1.99 (m, 2H), 1.95−1.85 (m, 2H), 1.77−1.67 (m, 1H). HRMS (ESI) m/z: $[M + H]^+$ calcd for $C_{24}H_{33}N_5O_2S_3{}^{185}Re$, 704.1326; found, 704.1323. HPLC retention time: 6.27 min, 98.9%.

*2-((5-((2-(6-(Dimethylamino)pyridin-3-yl)benzo[d]thiazol-6-yl)oxy)pentyl)(2-((2-mercaptoethyl)amino)ethyl)amino)-ethane-1-thiol-rhenium(V) oxide (**15c**).* Yield, 41%; mp 212.2−213.5 °C. ^{1}H NMR (400 MHz, DMSO-d_6, δ): 8.72 (d, J = 2.2 Hz, 1H), 8.07 (dd, J = 8.9, 2.3 Hz, 1H), 7.84 (d, J = 8.9 Hz, 1H), 7.66 (d, J = 2.3 Hz, 1H), 7.09 (dd, J = 8.9, 2.3 Hz, 1H), 6.78 (d, J = 9.1 Hz, 1H), 4.18−3.98 (m, 4H), 3.97−3.77 (m, 2H), 3.64−3.56 (m, 1H), 3.49−3.42 (m, 1H), 3.41−3.29 (m, 2H), 3.28−3.16 (m, 2H), 3.13 (s, 6H), 3.08−2.97 (m, 1H), 2.73−2.61 (m, 2H), 1.93−1.75 (m, 4H), 1.73−1.62 (m, 1H), 1.55−1.43 (m, 2H). HRMS (ESI) m/z: $[M + H]^+$ calcd for $C_{25}H_{35}N_5O_2S_3{}^{187}Re$, 720.1511; found, 720.1500. HPLC retention time: 8.24 min, 96.5%.

*2-((6-((2-(6-(Dimethylamino)pyridin-3-yl)benzo[d]thiazol-6-yl)oxy)hexyl)(2-((2-mercaptoethyl)amino)ethyl)amino)-ethane-1-thiol-rhenium(V) oxide (**15d**).* Yield, 53%; mp 192.8−194.2 °C. ^{1}H NMR (400 MHz, $CDCl_3$, δ): 8.76 (d, J = 2.0 Hz, 1H), 8.15 (d, J = 8.9 Hz, 1H), 7.87 (d, J = 8.9 Hz, 1H), 7.32 (d, J = 2.5 Hz, 1H), 7.04 (dd, J = 8.9, 2.5 Hz, 1H), 6.60 (d, J = 9.0 Hz, 1H), 4.17−4.07 (m, 3H), 4.04 (t, J = 6.3 Hz, 2H), 3.90−3.75 (m, 2H), 3.60−3.50 (m, 1H), 3.42−3.31 (m, 3H), 3.29−3.22 (m, 1H), 3.19 (s, 6H), 3.06−2.93 (m, 2H), 2.77−2.70 (m, 1H), 1.91−1.78 (m, 4H), 1.75−1.66 (m, 1H), 1.64−1.56 (m, 2H), 1.52−1.40 (m, 2H). HRMS (ESI) m/z: $[M + H]^+$ calcd for $C_{26}H_{37}N_5O_2S_3{}^{185}Re$, 732.1639; found, 732.1638. HPLC retention time: 11.09 min, 99.3%.

*2-((2-((2-Mercaptoethyl)(3-((2-(6-(methylamino)pyridin-3-yl)benzo[d]thiazol-6-yl)oxy)propyl)amino)ethyl)amino)-ethane-1-thiol-rhenium(V) oxide (**16a**).* Yield, 40%; mp 231.5−232.5 °C. ^{1}H NMR (400 MHz, DMSO-d_6, δ): 8.62 (d, J = 2.3 Hz, 1H), 8.06−7.98 (m, 1H), 7.85 (d, J = 8.9 Hz, 1H), 7.70 (d, J = 2.5 Hz, 1H), 7.12 (dd, J = 8.9, 2.5 Hz, 1H), 6.64 (d, J = 8.9 Hz, 1H), 4.17 (t, J = 6.2 Hz, 2H), 4.15−4.04 (m, 3H), 3.89−3.80 (m, 1H), 3.65−3.50 (m, 3H), 3.31−3.17 (m, 3H), 3.10−3.00 (m, 1H), 2.87 (d, J = 3.0 Hz, 3H), 2.75−2.63 (m, 2H), 2.34−2.25 (m, 2H), 1.77−1.66 (m, 1H). HRMS (ESI) m/z: $[M + H]^+$ calcd for $C_{22}H_{29}N_5O_2S_3{}^{187}Re$, 678.1041; found, 678.1039. HPLC retention time: 5.12 min, 98.1%.

*2-((2-((2-Mercaptoethyl)(4-((2-(6-(methylamino)pyridin-3-yl)benzo[d]thiazol-6-yl)oxy)butyl)amino)ethyl)amino)-ethane-1-thiol-rhenium(V) oxide (**16b**).* Yield, 32%; mp 205.0−206.2 °C. ^{1}H NMR (400 MHz, $CDCl_3$, δ): 8.72 (d, J = 2.1 Hz, 1H), 8.12 (dd, J = 8.8, 2.3 Hz, 1H), 7.88 (d, J = 8.9 Hz, 1H), 7.33 (d, J = 2.3 Hz, 1H), 7.06 (dd, J = 8.9, 2.4 Hz, 1H), 6.48 (d, J = 8.8 Hz, 1H), 4.97 (d, J = 5.0 Hz, 1H), 4.24−4.06 (m, 5H), 3.95−3.85 (m, 1H), 3.83−3.75 (m, 1H), 3.70−3.59 (m, 1H), 3.47−3.32 (m, 3H), 3.31−3.23 (m, 1H), 3.07−2.96 (m, 5H), 2.78−2.70 (m, 1H), 2.12−1.99 (m, 2H), 1.95−1.84 (m, 2H), 1.78−1.71 (m, 1H). HRMS (ESI) m/z: $[M + H]^+$ calcd for $C_{23}H_{31}N_5O_2S_3{}^{185}Re$, 690.1170; found, 690.1176. HPLC retention time: 6.27 min, 99.4%.

*2-((2-((2-Mercaptoethyl)(5-((2-(6-(methylamino)pyridin-3-yl)benzo[d]thiazol-6-yl)oxy)pentyl)amino)ethyl)amino)-ethane-1-thiol-rhenium(V) oxide (**16c**).* Yield, 54%; mp 167.7−168.0 °C. ^{1}H NMR (400 MHz, $CDCl_3$, δ): 8.68 (d, J = 2.0 Hz, 1H), 8.16 (dd, J = 8.8, 2.3 Hz, 1H), 7.88 (d, J = 8.9 Hz, 1H), 7.32 (d, J = 2.5 Hz, 1H), 7.05 (dd, J = 8.9, 2.5 Hz, 1H), 6.52 (d, J = 8.8 Hz, 1H), 5.33 (s, 1H), 4.18−4.09 (m, 3H), 4.06 (t, J = 6.1 Hz, 2H), 3.92−3.83 (m, 1H), 3.82−3.76 (m, 1H), 3.63−3.54 (m, 1H), 3.44−3.32 (m, 3H), 3.30−3.21 (m, 1H), 3.06−2.95 (m, 5H), 2.79−2.71 (m, 1H), 1.97−1.84 (m, 4H), 1.77−1.68 (m, 1H), 1.66−1.56 (m, 2H). HRMS (ESI) m/z: $[M + H]^+$ calcd for $C_{24}H_{33}N_5O_2S_3{}^{185}Re$, 704.1326; found, 704.1313. HPLC retention time: 8.73 min, 98.4%.

*2-((2-((2-Mercaptoethyl)(6-((2-(6-(methylamino)pyridin-3-yl)benzo[d]thiazol-6-yl)oxy)hexyl)amino)ethyl)amino)-ethane-1-thiol-rhenium(V) oxide (**16d**).* Yield, 40%; mp 210.0−211.1 °C. ^{1}H NMR (400 MHz, $CDCl_3$, δ): 8.70 (d, J = 1.9 Hz, 1H), 8.14 (dd, J = 8.8, 2.3 Hz, 1H), 7.88 (d, J = 8.9 Hz, 1H), 7.32 (d, J = 2.5 Hz, 1H), 7.05 (dd, J = 8.9, 2.5 Hz, 1H), 6.50 (d, J = 8.8 Hz, 1H), 5.16 (s, 1H), 4.17−4.08 (m, 3H), 4.04 (t, J = 6.2 Hz, 2H), 3.90−3.75 (m, 2H), 3.61−3.51 (m, 1H), 3.43−3.31 (m, 3H), 3.29−3.21 (m, 1H), 3.06−2.94 (m, 5H), 2.77−2.70 (m, 1H), 1.91−1.77 (m, 4H), 1.74−1.66 (m, 1H), 1.65−1.56 (m, 2H), 1.52−1.42 (m, 2H). HRMS (ESI) m/z: $[M + H]^+$ calcd for $C_{25}H_{35}N_5O_2S_3{}^{185}Re$, 718.1483; found, 718.1498. HPLC retention time: 12.20 min, 99.6%

In Vitro Binding Assay Using Aggregated Aβ_{1-42} Peptides. Aβ_{1-42} aggregates were prepared according to procedures described previously.[19,23] The Aβ_{1-42} peptides (trifluoroacetate form, 0.53 mg) were dissolved in 2.4 mL of

DOI: 10.1021/acs.bioconjchem.6b00444
Bioconjugate Chem. XXXX, XXX, XXX−XXX

buffer solution (10 mM NaH_2PO_4 and 1 mM EDTA, pH = 7.4) and incubated at 37 °C for 42 h with constant and gentle shaking.

Competitive binding assays were performed in 12 mm × 75 mm borosilicate glass tubes (Fisher) following the procedure below. Aβ_{1-42} aggregates (100 μL) were added to a mixture containing 100 μL of [^{125}I]IMPY (approximately 100 000 cpm), 100 μL of Re complexes (10^{-4} to $10^{-9.5}$ M in ethanol), and 700 μL of bovine serum albumin solution (0.1% in water). The resulting mixture was incubated at 37 °C for 2 h and filtered through Whatman GF/B filters on a Mp-48T cell harvester (Brandel, Gaithersburg, MD) to separate the bound and free radioactive fractions. The filter sections containing bound [^{125}I]IMPY were detected using a γ-counter (WALLAC/Wizard 1470). Half-maximal inhibitory concentrations (IC_{50}) were calculated with GraphPad Prism 4.0, after which inhibition constant (K_i) values were calculated by the Cheng−Prusoff equation: $K_i = IC_{50}/(1 + [L]/K_d)$.[35]

In Vitro Fluorescent Staining of Aβ Plaques in Tg Mouse and AD Brains. Paraffin-embedded brain slices from Tg mice (APPswe/PSEN1, male, 12 months, 6 μm) and AD patients (8 μm) were prepared for fluorescent staining. The brain slices were deparaffinized in xylene for 2 × 20 min, washed in 100% ethanol for 2 × 5 min, washed in 90% ethanol−water for 5 min, washed in 80% ethanol−water for 5 min, washed in 60% ethanol−water for 5 min, washed in fresh water for 10 min, and incubated in PBS (0.2 M, pH = 7.4) for 30 min.

Brain slices were incubated in a 1.0 μM solution (10% ethanol−water) of Re complexes for 10 min and washed with 50% ethanol−water and PBS (0.2 M, pH = 7.4) for 5 min each. Fluorescent observation was performed on an Axio Observer Z1 inverted fluorescence microscope (Zeiss, Germany) using a DAPI filter set (excitation, 405 nm). To confirm the localization of Aβ plaques, adjacent brain slices from Tg mice were stained by thioflavin-S (1.0 μM) using a similar method.

Radiochemistry. [^{99m}Tc]GH was prepared by adding fresh $Na^{99m}TcO_4$ solution (1 mL) to GH kit (containing 8.0 mg glucoheptonate) and keeping it at room temperature for 10 min. Trifluoroacetic acid (100 μL) was added to a vial containing a precursor (0.1 mg), which was kept at room temperature for 10 min, after which 2 μL of triethylsilane was added to the resulting solution. After 10 min, the solvent was removed by nitrogen gas. The residue was dissolved in ethanol (100 μL) and transferred into [^{99m}Tc]GH solution. The mixture was heated at 100 °C for 10 min, cooled to room temperature, and purified via HPLC on a Venusil MP C18 column (Bonna-Agela Technologies, 5 μm, 4.6 × 250 mm) with acetonitrile−water (70%:30%) at a flow rate of 1 mL/min. The desired fraction was collected in a vial. Acetonitrile was removed using rotary evaporation. The final products were kept in saline containing 10% ethanol.

The ^{99m}Tc-labeled products were identified by retention time comparison using the corresponding rhenium complexes (Figure S3) on a Venusil MP C18 column (Bonna-Agela Technologies, 5 μm, 4.6 × 250 mm) with acetonitrile−water (80%:20%) at a flow rate of 1 mL/min. The chromatographic data also demonstrated radiochemical purity higher than 95%. In vitro stability assay was conducted in saline and mice serum according to procedures described previously.[28]

In Vitro Autoradiography. Brain slices from transgenic mice were prepared using the same procedures that were used for fluorescent staining and incubated in purified ^{99m}Tc-labeled ligands (100 μL, 10 μCi) for 1 h. After being washed with 40% ethanol−water for 5 min, the slices were exposed to a phosphorus plate (PerkinElmer) for 1 h. The autoradiographic images were acquired on a storage phosphor system (PerkinElmer) with 600 dpi resolution. To confirm specific binding, the same brain slices were fluorescent-stained by DANIR-3b afterward.

Biodistribution in Normal Mice. A solution of purified ^{99m}Tc-labeled ligands (100 μL, 5 μCi, 10% EtOH) in saline was administered intravenously to four groups of ICR mice (18−22 g, male, n = 5), which were sacrificed at 2, 10, 30, and 60 min post-injection. Organs of interest were removed, weighed, and subjected to a γ-counter (WALLAC/Wizard 1470). The results were expressed as a percentage of the injected dose per gram (% ID/g) of blood or organ.

Ex Vivo Autoradiography. A Tg mouse and an age-matched wild-type mouse received injections of [^{99m}Tc]**14b** (1.0 mCi in saline containing 10% ethanol) via the tail vein. The mice were sacrificed 30 min post-injection. The brains were removed immediately, embedded in optimal cutting temperature compound, frozen at −20 °C, and cut into 20 μm thick sections. After drying, the brain sections were exposed to imaging plates for 12 h and scanned with a storage phosphor system. The same brain sections were then stained with thioflavin-S to verify the presence of Aβ plaques.

In Vivo SPECT−CT Imaging in Rhesus Monkeys. Rhesus monkeys were anesthetized with ketamine (0.1 mL/kg) in combination with Sumianxin-II (0.1 mL/kg) via intramuscular injection and positioned on the bed of a SPECT−CT scanner. After intravenous administration of [^{99m}Tc]**14b** (10 mCi in 2 mL of saline containing 10% ethanol), the scan protocol was carried out immediately. During the scanning, a sealed plastic tube containing 20 μCi of [^{99m}Tc]**14b** (0.2% ID) was attached near the head as a radioactivity reference. After four successive sessions of head scanning (4 × 10 min), a whole-body scan was performed (approximately 20 min). All SPECT images were then merged with CT images. Brain regions were manually drawn on CT images and transferred to the corresponding SPECT images. Brain uptake was calculated by comparing the total counts of the brain regions to the counts of the radioactivity reference for quantitation, expressed as a percentage of the injected dose (% ID).

■ ASSOCIATED CONTENT

Supporting Information

The Supporting Information is available free of charge on the ACS Publications website at DOI: 10.1021/acs.bioconjchem.6b00444.

Figures showing in vitro fluorescent staining of Aβ plaques, HPLC co-injection profiles of ^{99m}Tc-labeled tracers, Stability results of [^{99m}Tc]**14b** in saline and mice serum, and in vitro autoradiography on the brain slices of Tg mice. A table showing biodistribution of radioactivity in normal ICR mice after intravenous injection of ^{99m}Tc-labeled tracers. NMR and MS spectra for precursors and rhenium complexes. (PDF)

■ AUTHOR INFORMATION

Corresponding Authors

*Z.L. e-mail: zg_liang1972@sina.com.

*B.C. e-mail: baianchen@ccmu.edu.cn.

DOI: 10.1021/acs.bioconjchem.6b00444
Bioconjugate Chem. XXXX, XXX, XXX−XXX

*M.C. e-mail: cmc@bnu.edu.cn.

Notes

The authors declare no competing financial interest.

■ ACKNOWLEDGMENTS

This work was funded by the National Natural Science Foundation of China (grant nos. 21571022 and 81571230) and the National Science and Technology Major Projects for Major New Drugs Innovation and Development (grant no. 2014ZX09507007-002). This work was also supported by the science and technology project of Beijing Municipal Education Commission (grant no. KM201310025002311722293) and Beijing Municipal Administration of Hospitals Incubating Program (grant no. PX2016016). We thank Dr. Jin Liu (College of Life Science, Beijing Normal University) for assistance with in vitro fluorescent staining.

■ ABBREVIATIONS USED

AD, Alzheimer's disease; Aβ, β-amyloid; PET, positron emission tomography; SPECT, single-photon emission computed tomography; BAT, bis(aminoethanethiol); Tg, transgenic; Cp, cyclopentadienyl; BBB, blood−brain barrier; FDA, Food and Drug Administration; IMPY, 4-(6-iodoimidazo[1,2-*a*]pyridin-2-yl)-*N*,*N*-dimethylaniline; Boc, *t*-butyloxy carbonyl; Tr, triphenylmethyl; TFA, trifluoroacetic acid; SD, standard deviation; GH, glucoheptonate; rt, room temperature; ID, injected dose; p.i., post injection; NMR, nuclear magnetic resonance; TMS, tetramethyl silane; *J*, coupling constant (in NMR spectrometry); MS, mass spectrometry; ESI, electrospray ionization; HRMS, high-resolution mass spectrometry; HPLC, high-performance liquid chromatography; DMSO, dimethyl sulfoxide; EDTA, ethylenediaminetetraacetic acid; PBS, phosphate-buffered saline

■ REFERENCES

(1) Scheltens, P., Blennow, K., Breteler, M. M. B., de Strooper, B., Frisoni, G. B., Salloway, S., and Van der Flier, W. M. (2016) Alzheimer's disease. *Lancet 388*, 505−517.

(2) Chan, K. Y., Wang, W., Wu, J. J., Liu, L., Theodoratou, E., Car, J., Middleton, L., Russ, T. C., Deary, I. J., Campbell, H., et al. (2013) Epidemiology of Alzheimer's disease and other forms of dementia in China, 1990−2010: a systematic review and analysis. *Lancet 381*, 2016−2023.

(3) Prince, M., Wimo, A., Guerchet, M., Ali, G.-C., Wu, Y.-T., and Prina, M. (2015) *World Alzheimer Report 2015*, Alzheimer's Disease International, London.

(4) Bolognesi, M. L., Gandini, A., Prati, F., and Uliassi, E. (2016) From Companion Diagnostics to Theranostics: A New Avenue for Alzheimer's Disease? *J. Med. Chem. 59*, 7759−7770.

(5) Bateman, R. (2015) Alzheimer's disease and other dementias: advances in 2014. *Lancet Neurol. 14*, 4−6.

(6) Hardy, J., and Selkoe, D. J. (2002) The Amyloid Hypothesis of Alzheimer's Disease: Progress and Problems on the Road to Therapeutics. *Science 297*, 353−356.

(7) Kung, H. F. (2012) The β-Amyloid Hypothesis in Alzheimer's Disease: Seeing Is Believing. *ACS Med. Chem. Lett. 3*, 265−267.

(8) Cui, M. (2013) Past and Recent Progress of Molecular Imaging Probes for beta-Amyloid Plaques in the Brain. *Curr. Med. Chem. 21*, 82−112.

(9) Herholz, K., and Ebmeier, K. (2011) Clinical amyloid imaging in Alzheimer's disease. *Lancet Neurol. 10*, 667−670.

(10) Yang, L., Rieves, D., and Ganley, C. (2012) Brain Amyloid Imaging - FDA Approval of Florbetapir F18 Injection. *N. Engl. J. Med. 367*, 885−887.

(11) Vandenberghe, R., Van Laere, K., Ivanoiu, A., Salmon, E., Bastin, C., Triau, E., Hasselbalch, S., Law, I., Andersen, A., Korner, A., et al. (2010) F-18-Flutemetamol Amyloid Imaging in Alzheimer Disease and Mild Cognitive Impairment A Phase 2 Trial. *Ann. Neurol. 68*, 319−329.

(12) Barthel, H., Gertz, H.-J., Dresel, S., Peters, O., Bartenstein, P., Buerger, K., Hiemeyer, F., Wittemer-Rump, S. M., Seibyl, J., Reininger, C., et al. (2011) Cerebral amyloid-beta PET with florbetaben (F-18) in patients with Alzheimer's disease and healthy controls: a multicentre phase 2 diagnostic study. *Lancet Neurol. 10*, 424−435.

(13) Ono, M., and Saji, H. (2015) Recent advances in molecular imaging probes for β-amyloid plaques. *MedChemComm 6*, 391−402.

(14) Newberg, A. B., Wintering, N. A., Plössl, K., Hochold, J., Stabin, M. G., Watson, M., Skovronsky, D., Clark, C. M., Kung, M.-P., and Kung, H. F. (2006) Safety, Biodistribution, and Dosimetry of ^{123}I-IMPY: A Novel Amyloid Plaque Imaging Agent for the Diagnosis of Alzheimer's Disease. *J. Nucl. Med. 47*, 748−754.

(15) Maya, Y., Okumura, Y., Kobayashi, R., Onishi, T., Shoyama, Y., Barret, O., Alagille, D., Jennings, D., Marek, K., Seibyl, J., et al. (2016) Preclinical properties and human in vivo assessment of ^{123}I-ABC577 as a novel SPECT agent for imaging amyloid-beta. *Brain 139*, 193−203.

(16) Bartholomä, M. D., Louie, A. S., Valliant, J. F., and Zubieta, J. (2010) Technetium and Gallium Derived Radiopharmaceuticals: Comparing and Contrasting the Chemistry of Two Important Radiometals for the Molecular Imaging Era. *Chem. Rev. 110*, 2903−2920.

(17) Jia, J., Cui, M., Dai, J., and Liu, B. (2015) 2-Phenylbenzothiazole conjugated with cyclopentadienyl tricarbonyl [CpM(CO)$_3$] (M = Re, ^{99m}Tc) complexes as potential imaging probes for beta-amyloid plaques. *Dalton Trans. 44*, 6406−6415.

(18) Yang, Y., Cui, M., Jin, B., Wang, X., Li, Z., Yu, P., Jia, J., Fu, H., Jia, H., and Liu, B. (2013) ^{99m}Tc-labeled dibenzylideneacetone derivatives as potential SPECT probes for in vivo imaging of beta-amyloid plaque. *Eur. J. Med. Chem. 64*, 90−98.

(19) Cheng, Y., Ono, M., Kimura, H., Ueda, M., and Saji, H. (2012) Technetium-99m labeled pyridyl benzofuran derivatives as single photon emission computed tomography imaging probes for beta-amyloid plaques in Alzheimer's brains. *J. Med. Chem. 55*, 2279−2286.

(20) Han, H., Cho, C.-G., and Lansbury, P. T. (1996) Technetium Complexes for the Quantitation of Brain Amyloid. *J. Am. Chem. Soc. 118*, 4506−4507.

(21) Ly, J. V., Donnan, G. A., Villemagne, V. L., Zavala, J. A., Ma, H., O'Keefe, G., Gong, S. J., Gunawan, R. M., Saunder, T., Ackerman, U., et al. (2010) ^{11}C-PIB binding is increased in patients with cerebral amyloid angiopathy−related hemorrhage. *Neurology 74*, 487−493.

(22) Zhuang, Z. P., Kung, M. P., Hou, C., Ploessl, K., and Kung, H. F. (2005) Biphenyls labeled with technetium 99m for imaging beta-amyloid plaques in the brain. *Nucl. Med. Biol. 32*, 171−184.

(23) Li, Z., Cui, M., Dai, J., Wang, X., Yu, P., Yang, Y., Jia, J., Fu, H., Ono, M., Jia, H., et al. (2013) Novel cyclopentadienyl tricarbonyl complexes of ^{99m}Tc mimicking chalcone as potential single-photon emission computed tomography imaging probes for beta-amyloid plaques in brain. *J. Med. Chem. 56*, 471−482.

(24) Noel, S., Cadet, S., Gras, E., and Hureau, C. (2013) The benzazole scaffold: a SWAT to combat Alzheimer's disease. *Chem. Soc. Rev. 42*, 7747−7762.

(25) Ono, M., Ikeoka, R., Watanabe, H., Kimura, H., Fuchigami, T., Haratake, M., Saji, H., and Nakayama, M. (2010) Synthesis and evaluation of novel chalcone derivatives with ^{99m}Tc/Re complexes as potential probes for detection of beta-amyloid plaques. *ACS Chem. Neurosci. 1*, 598−607.

(26) Wang, X., Cui, M., Yu, P., Li, Z., Yang, Y., Jia, H., and Liu, B. (2012) Synthesis and biological evaluation of novel technetium-99m labeled phenylbenzoxazole derivatives as potential imaging probes for beta-amyloid plaques in brain. *Bioorg. Med. Chem. Lett. 22*, 4327−4331.

(27) Oya, S., Plössl, K., Kung, M.-P., Stevenson, D. A., and Kung, H. F. (1998) Small and Neutral Tc^{v}O BAT, Bisaminoethanethiol (N_2S_2) Complexes for Developing New Brain Imaging Agents. *Nucl. Med. Biol. 25*, 135−140.

DOI: 10.1021/acs.bioconjchem.6b00444
Bioconjugate Chem. XXXX, XXX, XXX−XXX

(28) Yang, Y., Cui, M., Zhang, X., Dai, J., Zhang, Z., Lin, C., Guo, Y., and Liu, B. (2014) Radioiodinated benzyloxybenzene derivatives: a class of flexible ligands target to beta-amyloid plaques in Alzheimer's brains. *J. Med. Chem. 57*, 6030−6042.
(29) Cui, M., Ono, M., Kimura, H., Liu, B., and Saji, H. (2011) Synthesis and structure-affinity relationships of novel dibenzylideneacetone derivatives as probes for beta-amyloid plaques. *J. Med. Chem. 54*, 2225−2240.
(30) Fu, H., Cui, M., Zhao, L., Tu, P., Zhou, K., Dai, J., and Liu, B. (2015) Highly Sensitive Near-Infrared Fluorophores for in Vivo Detection of Amyloid-β Plaques in Alzheimer's Disease. *J. Med. Chem. 58*, 6972−6983.
(31) Choi, S. R., Golding, G., Zhuang, Z., Zhang, W., Lim, N., Hefti, F., Benedum, T. E., Kilbourn, M. R., Skovronsky, D., and Kung, H. F. (2009) Preclinical properties of ^{18}F-AV-45: a PET agent for Abeta plaques in the brain. *J. Nucl. Med. 50*, 1887−1894.
(32) Zhuang, Z.-P., Kung, M.-P., Wilson, A., Lee, C.-W., Plössl, K., Hou, C., Holtzman, D. M., and Kung, H. F. (2003) Structure−Activity Relationship of Imidazo[1,2-a]pyridines as Ligands for Detecting β-Amyloid Plaques in the Brain. *J. Med. Chem. 46*, 237−243.
(33) Cui, M., Wang, X., Yu, P., Zhang, J., Li, Z., Zhang, X., Yang, Y., Ono, M., Jia, H., Saji, H., et al. (2012) Synthesis and evaluation of novel ^{18}F labeled 2-pyridinylbenzoxazole and 2-pyridinylbenzothiazole derivatives as ligands for positron emission tomography (PET) imaging of beta-amyloid plaques. *J. Med. Chem. 55*, 9283−9296.
(34) Stephenson, K. A., Chandra, R., Zhuang, Z., Hou, C., Oya, S., Kung, M., and Kung, H. F. (2007) Fluoro-pegylated (FPEG) Imaging Agents Targeting Aβ Aggregates. *Bioconjugate Chem. 18*, 238−246.
(35) Yung-Chi, C., and Prusoff, W. H. (1973) Relationship between the inhibition constant (Ki) and the concentration of inhibitor which causes 50% inhibition (I50) of an enzymatic reaction. *Biochem. Pharmacol. 22*, 3099−3108.

DOI: 10.1021/acs.bioconjchem.6b00444
Bioconjugate Chem. XXXX, XXX, XXX−XXX